國 立 交 通 大 學

電信工程學系碩士班
碩士論文

用於多輸入多輸出正交分頻多工系統之
波束形成輔助多用戶適應性無線電資源管理技術

Beamforming Aided Multiuser Adaptive Radio Resource Management for MIMO-OFDM Systems

研 究 生：蕭清文　　Student: Ching-Wen Hsiao

指導教授：李大嵩 博士　　Advisor: Dr. Ta-Sung Lee

中 華 民 國 九 十 五 年 六 月

用於多輸入多輸出正交分頻多工系統之
波束形成輔助多用戶適應性無線電資源管理技術

Beamforming Aided Multiuser Adaptive Radio Resource Management for MIMO-OFDM Systems

研 究 生：蕭清文　　Student: Ching-Wen Hsiao

指導教授：李大嵩 博士　　Advisor: Dr. Ta-Sung Lee

國立交通大學

電信工程學系碩士班

碩士論文

A Thesis
Submitted to Institute of Communication Engineering
College of Electrical Engineering and Computer Science
National Chiao Tung University
in Partial Fulfillment of the Requirements
for the Degree of
Master of Science
in
Communication Engineering
June 2006
Hsinchu, Taiwan, Republic of China

中 華 民 國 九 十 五 年 六 月

用於多輸入多輸出正交分頻多工系統之波束形成輔助多用戶適應性無線電資源管理技術

學生：蕭清文　　指導教授：李大嵩 博士

國立交通大學電信工程學系碩士班

摘要

多輸入多輸出(Multiple-Input Multiple-Output, MIMO)為使用多天線於傳送和接收端的可靠通訊技術，並被認為是符合第四代高速通訊需求的最佳方案之一，透過空間多工的方式，多輸入多輸出技術可在空間中的獨立平行通道傳送不同資料串流，藉以提昇系統的整體傳輸速率。另一方面，正交分頻多工（Orthogonal Frequency Division Multiplexing, OFDM）為一種具高頻譜效益，並能有效克服多路徑衰落效應的調變技術。在本論文中，吾人將探討結合多輸入多輸出技術與多用戶正交分頻多工系統的通訊系統架構。基於相同副載波對於不同用戶會展現不同通道條件的現象，吾人將針對多用戶正交分頻多工系統提出一種動態副載波配置演算法，此演算法考慮個別用戶對於服務品質與傳輸速率不同的需求，配置一組最適當的副載波給每一用戶，藉以提昇系統的整體傳輸速率，並藉由波束形成技術，使用多用戶能在不干擾彼此的情況下，同時在相同的副載波傳送。此外，吾人更進一步針對多用戶多輸入多輸出正交分頻多工系統提出一種適應性傳收架構及位元負載演算法，使系統能夠隨時間動態地在頻率與空間通道上調整傳輸參數—例如，調變階數與傳輸能量—以便充分地利用空間、時間以及頻率通道上的特性以維持系統的目標錯誤率和各用戶的傳輸速率要求，同時更進一步有效降低系統所需要傳送能量。最後，吾人藉由電腦模擬驗證上述架構在多用戶無線通訊環境中具有優異的傳輸表現。

Beamforming Aided Multiuser Adaptive Radio Resource Management for MIMO-OFDM Systems

Student: Ching-Wen Hsiao Advisor: Dr. Ta-Sung Lee

Institute of Communication Engineering

National Chiao Tung University

Abstract

Multiple-input multiple-output (MIMO) is a promising technique suited to the increasing demand for high-speed 4G broadband wireless communications. Through spatial multiplexing, the MIMO technology can transmit multiple data streams in independent parallel spatial channels, hence increase the total transmission rate of the system. On the other hand, orthogonal frequency division multiplexing (OFDM) is a high spectral efficiency modulation technique that can efficiently deal with multipath fading effects especially suited to multiuser systems. In this thesis, a new wireless communication system called the multiuser MIMO-OFDM system is considered. Based on the fact that the same subcarrier experiencing different channel conditions for different users, a dynamic subcarrier allocation algorithm is proposed. This algorithm enhances the overall transmission rate of the system by allocating the most appropriate subcarriers to each user under the constraints of user-specific quality of service (QoS). In addition, by using beamforming techniques, we also allow users to occupy the same subcarrier at the same time without interfering each other. It results in system performance enhancement. Then, an adaptive multiuser MIMO-OFDM transceiver architecture along with a bit loading algorithm is proposed, which dynamically adjusts the transmission parameters such as modulation order and transmit power over spatial and frequency channels, to fully exploit the properties of the space-time-frequency channels to meet the target bit error rate (BER) and each user's rate requirement and further reduce the overall transmission power of the system. Finally, the performance of the proposed systems is evaluated by computer simulations, confirming that they work well in multiuser wireless communication environments.

Acknowledgement

I would like to express my deepest gratitude to my advisor, Dr. Ta-Sung Lee, for his enthusiastic guidance and great patience. I learned a lot from his positive attitude in many areas. Heartfelt thanks are also offered to all members in the Communication System Design and Signal Processing (CSDSP) Lab for their constant encouragement and help. Finally, I would like to show my sincere thanks to my parents for their inspiration and invaluable love.

Contents

List of Figures

List of Tables

Acronym Glossary

ADC	analog-to-digital conversion
AWGN	additive white Gaussian noise
BER	bit error rate
BLAST	Bell Lab Layered space time
BPSK	binary phase shift keying
BS	base station
CCI	co-channel interference
CNR	channel gain-to-noise ratio
CP	cyclic prefix
CRC	cyclic redundancy check
CSI	channel state information
D-BLAST	diagonal Bell labs' layered space-time
DFT	discrete Fourier transform
FDMA	frequency division multiple access
FFT	fast Fourier transform
FSK	frequency shift keying
ICI	intercarrier interference
IEEE	institute of electrical and electronics engineers
IFFT	inverse fast Fourier transform
ISI	intersymbol interference
LOS	line of sight
MAI	multiple access interference
MCM	multicarrier modulation

MIMO	multiple-input multiple-output
MISO	multiple-input single-output
MMSE	minimum mean square error
MS	mobile station
OFDM	orthogonal frequency division multiplexing
QAM	quadrature amplitude modulation
QoS	quality of service
QPSK	quaternary phase shift keying
RF	radio frequency
SD	spatial diversity
SIMO	single-input multiple-output
SISO	single-input single-output
SM	spatial multiplexing
SNR	signal-to-noise ratio
STC	space-time coding
SVD	singular value decomposition
TDD	time division duplex
TDMA	time division multiple access
V-BLAST	vertical Bell laboratory layered space-time
WF	water filling
ZF	zero forcing

Notations

$\bar{b}$	number of bits can be assigned in the system
B	total number of assigned bits
B_{req}	rate requirement per OFDM system
C	channel capacity
E_b	bit energy
E_s	symbol energy
$h_{i,j}$	channel gain between the jth transmit and ith receive antenna
$\mathbf{H}$	channel matrix
K	number of users in one cell
M	modulation order
N	number of subcarriers
N_{cp}	number of guard interval samples
N_t	number of transmit antenna
N_r	number of receive antenna
P	allocated power
T_s	symbol duration
T_{sample}	sampling period
$\mathbf{w}_R$	receive beamforming vector
$\mathbf{w}_T$	transmit beamforming vector
σ_n^2	noise power
δ	subcarrier indicator
λ	eigenvalue

Chapter 1

Introduction

The increasing popularity of enhanced communication services, such as wireless multimedia, telecommuting, fast Internet access, and video conferencing, has promoted the growing demand of high data rate, high mobility, and high quality of service (QoS) requirements for users. However, the limited available bandwidth drives the wireless communication technology towards the emerging issue of high spectral efficiency. Besides, in wireless channels, the time-selective and frequency-selective fading caused by multipath propagation, carrier frequency/phase shift, and Doppler shift limit the developments of high data rate and reliable communications. As a remedy, some efficient modulation and coding schemes such as coded multicarrier modulation, multiple-input multiple-output (MIMO) technology [1]-[11], and adaptive resource allocation [12]-[14] are proposed to enhance the spectral efficiency and quality of wireless communication links.

MIMO systems, which use multiple antennas at both transmitter and receiver, provide spatial diversity that can be used to mitigate signal-level fluctuations in fading channels [1]-[3]. In narrowband channels, MIMO systems can provide a diversity advantage in proportion to the product of the number of transmit and receive antennas. When the channel is unknown to the transmitter, diversity can be obtained by using

space-time codes [1]-[3]. When channel state information (CSI) is available at the transmitter, however, diversity can be obtained using a simple approach known as transmit beamforming and receive combining [4]-[11]. Compared with space-time codes, beamforming and combining achieves the same diversity order as well as additional array gain; thus, it can significantly improve system performance. This approach, however, requires knowledge of the transmit beamforming vector at the transmitter. When the uplink and downlink channels are not reciprocal (as in a frequency division duplexing system), the receiver informs the transmitter about the desired transmit beamforming vector through a feedback channel.

The high data rate wireless transmission over the multipath fading channels is mainly limited by intersymbol interference (ISI). Orthogonal frequency division multiplexing (OFDM) [17]-[18] has been considered as a reliable technology to deal with the ISI problem. The principle of the OFDM technology is to split a high data rate stream into a number of low data rate streams which are simultaneously transmitted on a number of orthogonal subcarriers. By adding a cyclic prefix (CP) to each OFDM symbol, both intersymbol and intercarrier interference can be removed and the channel also appears to be circular if the CP length is longer than the channel length. The multicarrier property of OFDM systems can not only improve the immunity to fast fading channels, but also make multiple access possible because the subcarriers are independent of each other.

OFDM combining antenna arrays at both the transmitter and receiver, which leads to a MIMO-OFDM configuration, can significantly increase the diversity gain or enhance the system capacity over time-variant and frequency-selective channels. Typical MIMO-OFDM systems can be categorized into two types: those based on spatial multiplexing (SM), [16] and those based on spatial diversity (SD) schemes. The former system is a layered spatial transmission scheme, in which different data streams

are transmitted from different transmit antennas simultaneously and received through nulling or canceling to mitigate the co-channel interference (CCI). The latter one uses beamforming techniques to improve the transmission reliability. Beamforming can provide power gain and increase the effective transmission rate without sacrificing the bandwidth.

In the multiuser MIMO-OFDM system, each of the multiple users' signals may undergo independent fading due to different locations of users. Therefore, the subcarriers in deep fade for one user may not be in the same fade for other users. In fact, it is quite unlikely that a subcarrier will be in deep fade for all users. By beamforming technique, the system can allow multiple users to occupy the same subcarrier without interfering each other. Hence, for a specific subcarrier, the groups of users with the best channel quality can use the subcarrier to transmit data yielding multiuser diversity effects [19]. Recently, methods for dynamically assigning subcarriers to each user have been widely investigated [20]-[21]. These dynamic subcarrier allocation algorithms can be geared to decrease the power consumption for a given achievable data rate or to increase the data rate when the available power is limited. In this thesis, a beamforming aided dynamic subcarrier allocation algorithm suited to the multiuser MIMO-OFDM system is developed to take both user-specific data rate and BER requirements into account and allocate to each user the most appropriate subcarriers with ZF beamforming.

As the instantaneous channel state information (CSI) is determined beforehand, the multiuser MIMO-OFDM system incorporating the adaptive modulation technique can provide a significant performance improvement. Adaptive modulation can dynamically adjust transmission parameters to alleviate the effects of channel impairments. Subcarriers with good channel qualities can employ higher modulation order to carry more bits per OFDM symbol, while subcarriers in deep fade may

employ lower modulation order or even no transmission. In addition, the adaptive modulation technique must take into account the additional signaling dimensions explored in future broadband wireless networks [15]. More specifically, the growing popularity of both MIMO and multiuser OFDM systems creates the demand for link adaptation solutions to integrate temporal, spectral, and spatial components together. In this thesis, an adaptive wireless transceiver called beamforming aided multiuser adaptive radio resource management is developed to effectively exploit the available degrees of freedom in wireless communication systems.

This thesis is organized as follows. In Chapter 2, the channel capacity and basic technique of a MIMO communication link are described first. Secondly the multiple access concepts of OFDM system is given. In Chapter 3, a beamforming aided subcarrier allocation algorithm is proposed which allows users to choose the most appropriate subcarriers according to their requirements and the channel qualities. This algorithm fully utilized the advantage of spatial diversity and power gain by beamforming and frequency diversity by subcarrier allocation. In Chapter 4, the adaptive modulation concepts are introduced and an optimal bit loading algorithm with low complexity suited to the multiuser MIMO-OFDM system is proposed to further decrease the total transmit power and still meet the target bit error rate (BER) and rate requirement. In Chapter 5, we combine the algorithm described in Chapter 3 and 4 which adaptively adjust the beamforming vectors, subcarrier, modulation orders and power for each user. Finally, Chapter 6 gives concluding remarks of this thesis and leads the way to some potential future works.

Chapter 2

MIMO-OFDM Technique Overview

Digital communication using multiple-input multiple-output (MIMO) has recently emerged as one of the most significant technical breakthroughs in wireless communications. The technology figures prominently on the list of recent technical advances with a chance of resolving the bottleneck of traffic capacity in future Internet intensive wireless networks.

In recent years, there has been substantial research interest in applying orthogonal frequency division multiplexing (OFDM) to high speed wireless communications due to its advantage in mitigating the severe effects of frequency-selective fading [22]-[23]. In this chapter, the basic ideas and key feature of MIMO–OFDM system will be introduced.

This Chapter focuses on the MIMO-OFDM techniques. An overview of the MIMO-OFDM system will first be given. Then we introduce MIMO techniques followed by introduction of MIMO-OFDM system which include the capacity, spatial multiplexing and diversity view. Finally OFDM technique is given in this chapter.

2.1 Introduction to MIMO-OFDM System

OFDM has long been regarded as an efficient approach to combat the adverse effects of multipath spread, and is the main solution to many wireless systems. It converts a frequency-selective channel into a parallel collection of frequency flat subchannels, which makes the receiver simpler. The time domain waveforms of the subcarriers are orthogonal, yet the signal spectrum corresponding to the different subcarriers overlap in frequency domain. Therefore, the available bandwidth is used very efficiently, especially compared with those systems having intercarrier guard bands, as shown in Figure 2.1. In order to eliminate inter-symbol interference (ISI) almost completely, a guard time is introduced for each OFDM symbol. Moreover, to eliminate inter-carrier interference (ICI), the OFDM symbol is further cyclically extended in the guard time, resulting in the cyclic prefix (CP). Otherwise, multipath remains an advantage for an OFDM system since the frequency selectivity caused by multipaths can improve the rank distribution of the channel matrices across those subcarriers, thereby increasing system capacity. We summarize the advantages of OFDM as follows [24]:

- High spectral efficiency
- Simple implementation by FFT
- Robustness against narrowband interference
- High flexibility in terms of link adaptation for having many subcarriers
- Suitability for high-data-rate transmission over a multipath fading channel

MIMO systems where multiple antennas are used at both the transmitter and receiver have been also acknowledged as one of the most promising techniques to achieve dramatic improvement in physical-layer performance [25], [26]. Moreover, the use of multiple antennas enables space-division multiple access (SDMA), which

allows intracell bandwidth reuse by multiplexing spatially separable users [27], [28]. Channel variation in the spatial domain also provides an inherent degree of freedom for adaptive transmission. To sum up, after OFDM is combined with MIMO techniques, MIMO-OFDM can be a potential candidate for the next generation wireless communication systems.

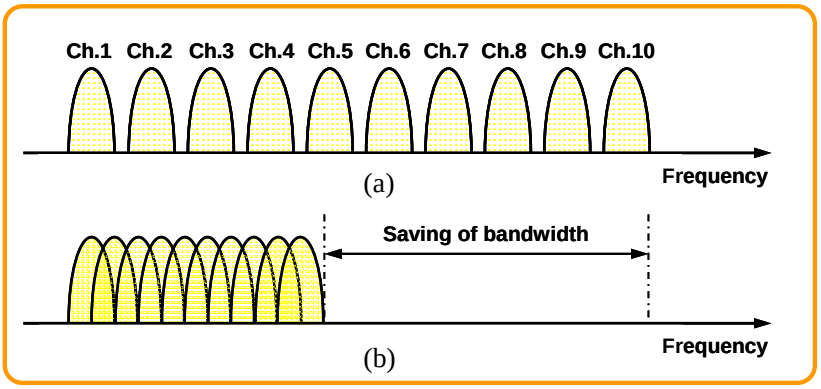

Figure 2.1: (I) Conventional multicarrier technique

(II) Orthogonal multicarrier modulation technique

2.2 Channel Capacity

A measure of how much information that can be transmitted and received with a negligible probability of error is called the channel capacity. To determine this measure of channel potential, a channel encoder receiving a source symbol every T_s second is assumed. If S represents the set of all source symbols and the entropy rate of the source is written as $H(s)$, the channel encoder will receive $H(s)/T_s$ information bits per second on average. A channel codeword leaving the channel encoder every T_c second is also assumed. In order to be able to transmit all the information from the source, there must be R information bits per channel symbol.

$$R = \frac{H(s)T_c}{T_s} \tag{2.1}$$

The number R is called the information rate of the channel encoder. The maximum information rate that can be used causing negligible probability of errors at the output is called the capacity of the channel. By transmitting information with the rate R, the channel is used every T_c seconds. The channel capacity is then measured in bits per channel use. Assuming that the channel has bandwidth W, the input and output can be represented by samples taken $T_s = 1/2W$ seconds apart. With a band-limited channel, the capacity is measured in information bits per second. It is common to represent the channel capacity within a unit bandwidth of the channel, which means that the channel capacity is measured in bits/sec/Hz.

It is desirable to design transmission schemes that exploit the channel capacity as much as possible. Representing the input and output of a memoryless wireless channel with the random variables X and Y respectively, the channel capacity is defined as

$$C = \max_{p(x)} I(X;Y) \quad \text{bits/sec/Hz} \tag{2.2}$$

where $I(X;Y)$ represents the mutual information between X and Y. Equation (2.2) states that the mutual information is maximized when considering all possible transmitter statistical distributions $p(x)$. Mutual information is a measure of the amount of information that one random variable contains about another one. The mutual information between X and Y can also be written as

$$I(X;Y) = H(Y) - H(Y|X) \tag{2.3}$$

where $H(Y|X)$ represents the conditional entropy between the random variables X and Y. The entropy of a random variable can be described as a measure of the uncertainty of the random variable. It can also be described as a measure of the amount of information required on average to describe the random variable. Due to Equation (2.3), mutual information can be described as the reduction in the uncertainty of one random variable due to the knowledge of the other. Note that the mutual information

between X and Y depends on the properties of X (through the probability distribution of X) and the properties of channel (through a channel matrix **H**). In the following, four different kinds of channel capacities are introduced (single-input single-output (SISO), single-input multiple-output (SIMO), multiple-input single-output (MISO), and MIMO) to get the further concepts about the properties of the channel capacity.

2.2.1 SISO Channel Capacity

The ergodic (mean) capacity of a random channel ($N_t = N_r = 1$) with the average transmit power constraint P_T can be expressed as

$$C = E_H \left\{ \max_{p(x):P \le P_T} I(X;Y) \right\} \quad \text{bits/sec/Hz} \tag{2.4}$$

where E_H denotes the expectation over all channel realizations and P is the average power of a single channel codeword transmitted over the channel. Compared to the definition in Equation (2.2), the capacity of the channel is now defined as the maximum of the mutual information between the input and output over all statistical distributions on the input that satisfy the power constraint. If each channel symbol at the transmitter is denoted by s, the average power constraint can be expressed as

$$P = E\left[|s|^2 \right] \le P_T \tag{2.5}$$

Using Equation (2.4), the ergodic (mean) capacity of a SISO system ($N_t = N_r = 1$) with a random complex channel gain h_{11} is given by

$$C = E_H \left\{ \log_2 \left(1 + \rho \cdot |h_{11}|^2 \right) \right\} \quad \text{bits/sec/Hz} \tag{2.6}$$

where ρ is the average signal-to-noise (SNR) ratio at the receive branch. If $|h_{11}|$ is Rayleigh, $|h_{11}|^2$ follows a chi-squared distribution with two degrees of freedom. Equation (2.6) can then be written as

$$C = E_H \left\{ \log_2 \left(1 + \rho \cdot \chi_2^2 \right) \right\} \quad \text{bits/sec/Hz} \tag{2.7}$$

where χ_2^2 is a chi-square distributed random variable with two degrees of freedom.

2.2.2 SIMO and MISO Channel Capacity

As more antennas deployed at the receiving end, the statistics of capacity improve. Then the ergodic (mean) capacity of a SIMO system with N_r receive antennas is given by

$$C = \log_2 (1 + \rho \sum_{i=1}^{N_r} |h_{i1}|^2) \quad \text{bits/sec/Hz} \tag{2.8}$$

where h_{i1} represents the gain for the receive antenna i. Note that the crucial feature in Equation (2.8) is that increasing the number of receive antennas N_r only results in a logarithmic increase in the ergodic (mean) capacity. Similarly, if transmit diversity is opted, in the common case, where the transmitter doesn't have the channel knowledge, the ergodic (mean) capacity of a MISO system with N_t transmit antennas is given by

$$C = \log_2 (1 + \frac{\rho}{N_t} \sum_{i=1}^{N_t} |h_{1i}|^2) \quad \text{bits/sec/Hz} \tag{2.9}$$

where the normalization by N_t ensures a fixed total transmit power and shows the absence of array gain in that case (compared to the case in Equation (2.8), where the channel energy can be combined coherently). Again, the capacity has a logarithmic relationship with the number of transmit antennas N_t.

2.2.3 MIMO Channel Capacity

The capacity of a random MIMO channel with the power constraint P_T can be expressed as

$$C = E_H \left\{ \max_{p(\mathbf{x}):tr(\Phi)\le P_T} I(\mathbf{x};\mathbf{y}) \right\} \quad \text{bits/sec/Hz} \tag{2.10}$$

where $\mathbf{\Phi} = E\{xx^H\}^2$ is the covariance matrix of the transmit signal vector **x**. By the relationship between mutual information and entropy and using Equation (2.1), Equation (2.10) can be expanded as follows for a given channel matrix **H**.

$$\begin{aligned} I(\mathbf{x};\mathbf{y}) &= h(\mathbf{y}) - h(\mathbf{y}\,|\,\mathbf{x}) \\ &= h(\mathbf{y}) - h(\mathbf{H}\mathbf{x} + \mathbf{n}\,|\,\mathbf{x}) \\ &= h(\mathbf{y}) - h(\mathbf{n}\,|\,\mathbf{x}) \\ &= h(\mathbf{y}) - h(\mathbf{n}) \end{aligned} \tag{2.11}$$

where $h(\cdot)$ denotes the differential entropy of a continuous random variable. It is assumed that the transmit vector **x** and the noise vector **n** are independent.

When **y** is Gaussian, Equation (2.11) is maximized. Since the normal distribution maximizes the entropy for a given variance. The differential entropy of a complex Gaussian vector $\mathbf{y} \in \mathbf{C}^n$, the differential entropy is less than or equal to $\log_2 \det(\pi e \mathbf{K})$, with equality if and only if **y** is a circularly symmetric complex Gaussian with $E\{yy^H\} = \mathbf{K}$. For a real Gaussian vector $\mathbf{y} \in \mathbf{R}^n$ with zero mean and covariance matrix, **K** is equal to $\log_2\left((2\pi e)^n \det \mathbf{K}\right)/2$. Assuming the optimal Gaussian distribution for the transmit vector **x**, the covariance matrix of the received complex vector **y** is given by

$$\begin{aligned} E\left\{\mathbf{y}\mathbf{y}^H\right\} &= E\left\{(\mathbf{H}\mathbf{x} + \mathbf{n})(\mathbf{H}\mathbf{x} + \mathbf{n})^H\right\} \\ &= E\left\{\mathbf{H}\mathbf{x}\mathbf{x}^H\mathbf{H}^H\right\} + E\left\{\mathbf{n}\mathbf{n}^H\right\} \\ &= \mathbf{H}\mathbf{\Phi}\mathbf{H}^H + \mathbf{K}^n \\ &= \mathbf{K}^d + \mathbf{K}^n \end{aligned} \tag{2.12}$$

The desired part and the noise part of Equation (2.12) denotes respectively by the superscript *d* and *n*. The maximum mutual information of a random MIMO channel is then given by

$$
\begin{aligned}
I &= h(\mathbf{y}) - h(\mathbf{n}) \\
&= \log_2\left[\det\left(\pi e\left(\mathbf{K}^d + \mathbf{K}^n\right)\right)\right] - \log_2\left[\det\left(\pi e\mathbf{K}^n\right)\right] \\
&= \log_2\left[\det\left(\mathbf{K}^d + \mathbf{K}^n\right)\right] - \log_2\left[\det\left(\mathbf{K}^n\right)\right] \\
&= \log_2\left[\det\left(\left(\mathbf{K}^d + \mathbf{K}^n\right)\left(\mathbf{K}^n\right)^{-1}\right)\right] \\
&= \log_2\left[\det\left(\mathbf{K}^d\left(\mathbf{K}^n\right)^{-1} + \mathbf{I}_M\right)\right] \\
&= \log_2\left[\det\left(\mathbf{H}\Phi\mathbf{H}^H\left(\mathbf{K}^n\right)^{-1} + \mathbf{I}_M\right)\right]
\end{aligned}
\tag{2.13}
$$

When the transmitter has no knowledge about the channel, it is optimal to use a uniform power distribution. The transmit covariance matrix is then given by $\Phi = P_T\mathbf{I}_{N_t} / N_t$. It is also common to assume uncorrelated noise in each receive antenna described by the covariance matrix $\mathbf{K}^n = \sigma^2\mathbf{I}_{N_r}$. The ergodic (mean) capacity for a complex additive white Gaussian noise (AWGN) MIMO channel can then be expressed as

$$
C = E_H\left\{\log_2\left[\det\left(\mathbf{I}_{N_r} + \frac{P_T}{\sigma^2 N_t}\mathbf{H}\mathbf{H}^H\right)\right]\right\} \text{ bits/sec/Hz} \tag{2.14}
$$

Equation (2.14) can also be written as

$$
C = E_H\left\{\log_2\left[\det\left(\mathbf{I}_{N_r} + \frac{\rho}{N_t}\mathbf{H}\mathbf{H}^H\right)\right]\right\} \text{ bits/sec/Hz} \tag{2.15}
$$

where $\rho = P_T / \sigma^2$ is the average signal-to-noise (SNR) at each receive antenna. By the law of large numbers, the term $\mathbf{H}\mathbf{H}^H / N_t \to \mathbf{I}_{N_r}$ as N_r is fixed and N_t gets large. Hence the capacity in the limit of large transmit antennas N_t can be written as

$$
C = E_H\left\{N_r \cdot \log_2(1+\rho)\right\} \text{ bits/sec/Hz} \tag{2.16}
$$

Further analysis of the MIMO channel capacity given in Equation (2.15) is possible by diagonalizing the product matrix $\mathbf{H}\mathbf{H}^H$ either by eigenvalue decomposition or singular value decomposition (SVD). By using SVD, the matrix

product is written as

$$\mathbf{H} = \mathbf{U}\boldsymbol{\Sigma}\mathbf{V}^H \tag{2.17}$$

where **U** and **V** are unitary matrices of left and right singular vectors respectively, and Σ is a triangular matrix with singular values on the main diagonal. All elements on the diagonal are zero except for the first *k* elements. The number of non-zero singular values *k* of Σ equals the rank of the channel matrix. Substituting Equation (2.17) into Equation (2.15), the MIMO channel capacity can be written as

$$C = E_H \left\{ \log_2 \left[\det \left(I_{N_r} + \frac{\rho}{N_t} \mathbf{U}\boldsymbol{\Sigma}\boldsymbol{\Sigma}^H \mathbf{U}^H \right) \right] \right\} \text{ bits/sec/Hz} \tag{2.18}$$

The matrix product $\mathbf{H}\mathbf{H}^H$ can also be described by using eigenvalue decomposition on the channel matrix **H** written as

$$\mathbf{H}\mathbf{H}^H = \mathbf{E}\boldsymbol{\Lambda}\mathbf{E}^H, \tag{2.19}$$

where **E** is the eigenvector matrix with orthonormal columns and $\boldsymbol{\Lambda}$ is a diagonal matrix with the eigenvalues on the main diagonal. Using this notation, Equation (2.15) can be written as

$$C = E_H \left\{ \log_2 \left[\det \left(\mathbf{I}_{N_r} + \frac{\rho}{N_t} \mathbf{E}\boldsymbol{\Lambda}\mathbf{E}^H \right) \right] \right\} \text{ bits/sec/Hz} \tag{2.20}$$

After diagonalizing the product matrix $\mathbf{H}\mathbf{H}^H$, the capacity formulas of the MIMO channel now includes unitary and diagonal matrices only. It is then easier to see that the total capacity of a MIMO channel is made up by the sum of parallel AWGN SISO subchannels. The number of parallel subchannels is determined by the rank of the channel matrix. In general, the rank of the channel matrix is given by

$$rank(\mathbf{H}) = k \le \min(N_t, N_r) \tag{2.21}$$

Using the fact that the determinant of a unitary matrix is equal to 1 and Equation (2.21), Equations (2.18) and (2.20) can be expressed respectively as

$$C = E_H \left\{ \sum_{i=1}^{k} \log_2 \left(1 + \frac{\rho}{N_t} \sigma_i^2 \right) \right\} \text{ bits/sec/Hz} \tag{2.22}$$

$$= E_H \left\{ \sum_{i=1}^{k} \log_2 \left(1 + \frac{\rho}{N_t} \lambda_i \right) \right\} \text{ bits/sec/Hz} \tag{2.23}$$

where σ_i^2 are the squared singular values of the diagonal matrix Σ and λ_i are the eigenvalues of the diagonal matrix $\mathbf{\Lambda}$. The maximum capacity of a MIMO channel is achieved in the unrealistic situation when each of the N_t transmitted signals is received by the same set of N_r antennas without interference. It can also be described as if each transmitted signal is received by a separate set of receive antennas, giving a total number of $N_t \cdot N_r$ receive antennas.

With optimal combining at the receiver and receive diversity only (N_r = 1), the channel capacity can be expressed as

$$C = E_H \left\{ \log_2 \left(1 + \rho \cdot \chi_{2N_r}^2 \right) \right\} \text{ bits/sec/Hz} \tag{2.24}$$

where $\chi_{2N_r}^2$ is a chi-distributed random variable with $2N_r$ degrees of freedom. If there are N_t transmit antennas and optimal combining between N_r antennas at the receiver, the capacity can be written as

$$C = E_H \left\{ N_t \cdot \log_2 \left(1 + \frac{\rho}{N_t} \cdot \chi_{2N_r}^2 \right) \right\} \text{ bits/sec/Hz} \tag{2.25}$$

Equation (2.25) represents the upper bound of a Rayleigh fading MIMO channel.

When the channel is known at the transmitter, the maximum capacity of a MIMO channel can be achieved by using the water-filling (WF) principle on the transmit covariance matrix. The capacity is then given by

$$
\begin{aligned}
C &= E_H \left\{ \sum_{i=1}^{k} \log_2 \left(1 + \varepsilon_i \frac{\rho}{N_t} \lambda_i \right) \right\} \\
&= E_H \left\{ \sum_{i=1}^{k} \log_2 \left(1 + \varepsilon_i \frac{\rho}{N_t} \sigma_i^2 \right) \right\} \\
&= \sum_{i=1}^{k} \log_2 (u \lambda_i)^+ \quad \text{bits/sec/Hz}
\end{aligned}
\tag{2.26}
$$

where "+" denotes taking only those terms which are positive and u is a scalar, representing the portion of the available transmit power going into the ith subchannel which is chosen to satisfy

$$
\rho = \sum_{i=1}^{k} (u - \lambda_i^{-1})^+ \tag{2.27}
$$

Since u is a complicated nonlinear function of $\lambda_1, \lambda_2, \ldots, \lambda_k$, the distribution of the channel capacity appears intractable, even in the Wishart case when the joint distribution of $\lambda_1, \lambda_2, \ldots, \lambda_k$ is known. Nevertheless, the channel capacity can be simulated using Equations (2.26) and (2.27) for any given $\mathbf{H}\mathbf{H}^H$ so that the optimal capacity can be computed numerically for any channel [29].

2.3 Diversity Based on MIMO Techniques

Antenna diversity, or spatial diversity, can be obtained by placing multiple antennas at the transmitter and/or the receiver. If the antennas are placed sufficiently far apart, the channel gains between different antennas pairs fade more independently, and independent signal paths are created. The required antenna separation depends on the local scattering environment as well as on the carrier frequency. For a mobile which is near the round with many scatterers around, the channel decorrelates over shorter spatial distances, and typical antenna separation of half to one carrier wavelength is sufficient. For base stations on high towers, larger antenna separation of several to 10's of wavelengths may be required.

We will look at both receive diversity, using multiple receive antennas (single-input, multi-output SIMO channels), and transmit diversity, using multiple transmit antennas (multi-input, single-output MISO channels). Interesting coding problems arise in the latter and have led to recent excitement in space-time codes.

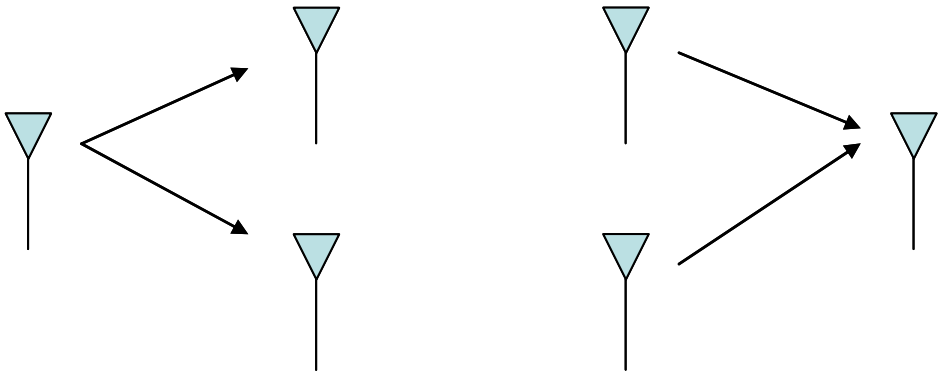

(I) (II)

Figure 2.2: (I) Receive diversity (II) Transmit diversity

2.3.1 Receive Diversity

In a flat fading channel with one transmit antenna and L receive antennas (Figure 2.2 (I)), the channel model is as follows:

$$y_l[m] = h_l[m]x[m] + w_l[m] \quad l = 1,...,L \tag{2.28}$$

where the noise $w_l[m] \sim CN(0, N_0)$ and independent across the antennas. We would like to detect $x[1]$ based on $y_1[1],..., y_L[1]$. This is exactly the same detection problem as in the use of a repetition cod over time, with L diversity branches now over space instead of over time. If the antennas are spaced sufficiently far apart, then we can assume that the gains $h_l[1]$ are independent Rayleigh, and we get a diversity gain of L.

With receive diversity, there are actually two types of gain as we increase L. this can be seen for the error probability of BPSK conditioned on the channel gains:

$$Q(\sqrt{2\|\mathbf{h}\|^2 \,\mathrm{SNR}}). \tag{2.29}$$

We can break up the total received SNR conditioned on the channel gains into a product of two terms:

$$\|\mathbf{h}\|^2 \text{SNR}=L\text{SNR}\cdot\frac{1}{L}\|\mathbf{h}\|^2. \tag{2.30}$$

The first term corresponds to a power gain (also called array gain): by having multiple receive antennas and coherent combining at the receiver, the effective total received signal power increases linearly with L: doubling L yields a 3 dB power gain. The second term reflects the diversity gain: by averaging over multiple independent signal paths, the probability that the overall gain is small is decreased. The diversity gain L is reflected in the SNR exponent; the power gain affects the constant before the $1/\text{SNR}^L$. Note that if the channel gains $h_l[1]$ are fully correlated across all branches, then we only get a power gain but no diversity gain as we increase *L*. on the other hand, even when all the h_l are independent there is a diminishing marginal return as *L* increases: due to the law of large numbers, the second term in (2.30),

$$\frac{1}{L}\|\mathbf{h}\|^2=\frac{1}{L}\sum_{l=1}^{L}|h_l[1]|^2, \tag{2.31}$$

Converges to 1 with increasing *L* (assuming each of the channel gains is normalized to have unit variance). The power gain, on the other hand, suffers from no such limitation: a 3 dB gain is obtained for every doubling of the number of antennas.

2.3.2 Transmit Diversity: Space-Time Codes

Now consider the case when there are *L* transmit antennas and one receive antenna, the MISO channel (Figure 2.2 (II)). This is common in the downlink of a cellular system since it is often cheaper to have multiple antennas at the base station than to having multiple antennas at every handset. It is easy to get a diversity gain of *L*: simply transmit the same symbol over the *L* different antennas during *L* symbol times. At any

one time, only one antenna is turned on and the rest are silent. This is simply a repetition code, and , as we have seen in the previous section, repetition codes are quite wasteful of degrees of freedom.

More generally, any time diversity code of block length L can be used on this transmit diversity system: simply use one antenna at a time and transmit the coded symbols of the time diversity code successively over the different antennas. This provides a coding gain over the repetition code. One can also design a code specifically for the transmit diversity system. There have been a lot of research activities in this area under the rubric of space-time coding and here we discuss the simplest, and yet one of the most elegant, space-time code which is called Alamouti scheme. This is the transmit diversity scheme proposed in several third-generation cellular standards. Alamouti scheme is designed for two transmit antennas; generalization to more than two antennas is possible, to some extent.

2.3.2.1 Alamouti Scheme

With flat fading, the two transmit, single receive channel is written as

$$y[m] = h_1[m]x_1[m] + h_2[m]x_2[m] + w[m] \tag{2.32}$$

where h_i is the channel gain from transmit antennas i. the Alamouti scheme transmits two complex symbols u_1 and u_2 over two symbol times: at time 1, $x_1[1]=u_1$, $x_2[1]=u_2$; at time 2, $x_1[2]= -u_2^*$, $x_2[1]= -u_1$. If we assume that the channel remains constant over the two symbol times and set $h_1=h_1[1]= h_1[2]$, $h_2=h_2[1]= h_2[2]$, then we can write the matrix form:

$$\begin{bmatrix} y[1] & y[2] \end{bmatrix} = \begin{bmatrix} h_1 & h_2 \end{bmatrix} \begin{bmatrix} u_1 & -u_2^* \\ u_2 & -u_1 \end{bmatrix} + \begin{bmatrix} w[1] & w[2] \end{bmatrix}. \tag{2.33}$$

We are interested in detecting u_1, u_2, so we rewrite this equation as

$$\begin{bmatrix} y[1] \\ y[2]^* \end{bmatrix} = \begin{bmatrix} h_1 & h_2 \\ h_2^* & -h_1^* \end{bmatrix} \begin{bmatrix} u_1 \\ u_2 \end{bmatrix} + \begin{bmatrix} w[1] \\ w[2]^* \end{bmatrix} \tag{2.34}$$

We observe that the columns of the square matrix are orthogonal. Hence, the detection problem for u_1,u_2 decomposes into two separate, orthogonal, scalar problems. We project y onto each of the two columns to obtain the sufficient statistics

$$r_i = \|\mathbf{h}\| u_i + w_i \quad i = 1, 2 \tag{2.35}$$

where $\mathbf{h} = [h_1, h_2]^t$ and $w_i \sim CN(0, N_0)$ and w_1, w_2 are independent. Thus, the diversity gain is 2 for the detection of each symbol. Compared to the repetition code, 2 symbols are now transmitted over two symbol times instead of 1 symbol, but with half the power in each symbol (assuming that the total transmit power is the same in both cases).

The Alamouti scheme works for any constellation for the symbols u_1, u_2, but suppose now they are BPSK symbols, thus conveying a total of two bits over two symbol times. In the repetition scheme, we need to use 4-PAM symbols to achieve the same data rate. To achieve the same minimum distance as the BPSK symbols in the Alamouti scheme, we need 5 times the energy per symbol. Take into account the factor of 2 energy saving since we are only transmitting one symbol at a time in the repetition scheme, we see that the repetition scheme requires a factor of 2.5 (4dB) more power than the Alamouti scheme. Again, the repetition scheme suffers from an inefficient utilization of the available degrees of freedom in the channel: over the two symbol times, bits are packed into only one dimension of the received signal space, namely along the direction $[h_1, h_2]^t$. In contrast, the Alamouti scheme spreads the information onto two dimensions- along the orthogonal directions $[h_1, h_2^*]^t$ and $[h_2, -h_1^*]^t$.

2.4 Spatial Multiplexing Based on MIMO Techniques

The use of multiple antennas at both ends of a wireless link has recently been shown to have the potential of achieving extraordinary data rate. The corresponding technology is known as spatial multiplexing [30]-[34]. It allows a data rate enhancement in a wireless radio link without additional power or bandwidth consumption. In spatial multiplexing systems, different data streams are transmitted from different transmit antennas simultaneously or sequentially and these data streams are separated and demultiplexed to yield the original transmitted signals according to their unique spatial signatures at the receiver. An illustration of the spatial multiplexing system is shown in Figure. 2.3. The separation step is made possible by the fact that the rich scattering multipath contributes to lower correlation between MIMO channel coefficients, and creates a desirable full rank and low condition number coefficient matrix condition to resolve N_t unknowns from a linear system of N_r equations. In the following, two typical spatial multiplexing schemes, D-BLAST [20] and V-BLAST [32], [33], are introduced.

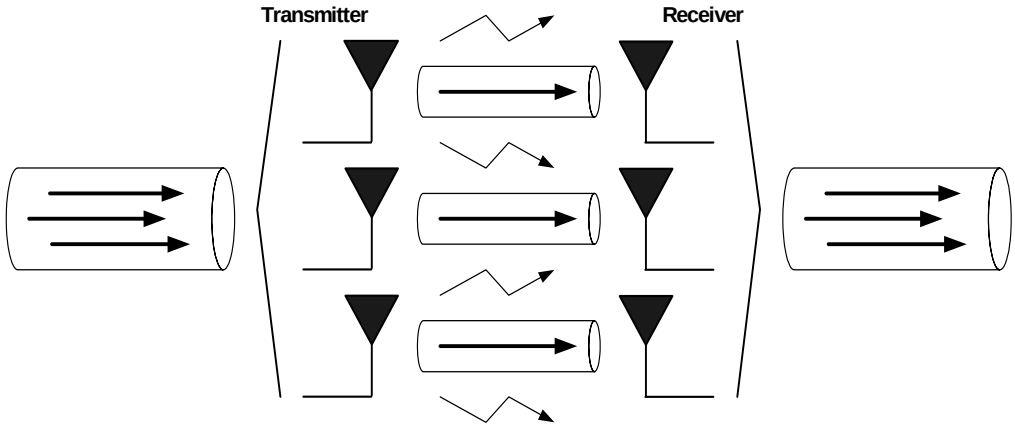

Figure 2.3: An illustration of a spatial multiplexing system

2.4.1 Diagonal Bell Lab's Layered Space-Time (D-BLAST)

Space-time coding (STC) performs channel coding across space and time to exploit the spatial diversity offered by MIMO systems to increase system capacity. However, the decoding complexity of the space-time codes is exponentially increased with the number of transmit antennas, which makes it hard to implement real-time decoding as the number of antennas grows. To reduce the complexity of space-time based MIMO systems, D-BLAST architecture has been proposed in [30]. Rather than try to achieve optimal channel coding scheme, in D-BLAST architecture, the input data stream is divided into several substreams. Each substream is encoded independently using an elegant diagonally-layered coding structure in which code blocks are dispersed across diagonals in space-time and the association of corresponding output stream with transmit antenna is periodically cycled to explore spatial diversity. To decode each layer, channel parameters are used to cancel interference from undetected signals to make the desired signal as "clean" as possible.

Figure 2.4 shows the typical encoding steps in D-BLAST. Considering a system with N_t transmit and N_r receive antennas, the high rate information data stream is first demultiplexed into N_t subsequences. Each subsequence is encoded by a conventional 1-D constituent code with low decoding complexity. The encoders apply these coded symbols to generate a semi-infinite matrix $\boldsymbol{C}$ of N_t rows to be transmitted. The element in the pth row and tth column of $\boldsymbol{C}$, c_t^p, is transmitted by the pth transmit antenna at time t. As illustrated in Figure. 2.3, $c_1^1, c_2^2, c_3^3, c_4^1, c_5^2, c_6^3$ are encoded by encoder α, $c_2^1, c_3^2, c_4^3, c_5^1, c_6^2, c_7^3$ are encoded by encoder β, and $c_3^1, c_4^2, c_5^3, c_6^1, c_7^2, c_8^3$ are encoded by encoder γ.

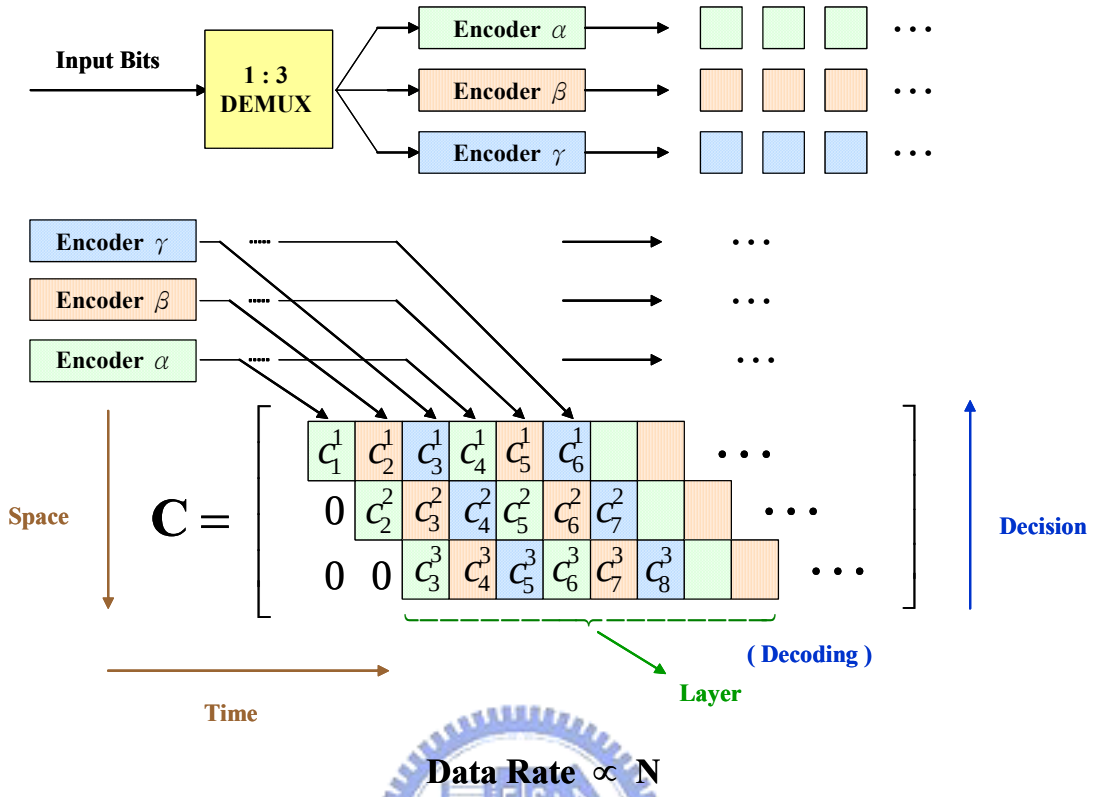

Figure 2.4: Diagonal Bell Labs' Layered Space-Time encoding procedure

Figure 2.5 shows the typical decoding steps of interference suppression, symbol detection, decoding, and interference cancellation performed in D-BLAST. The receiver generates decisions for the first diagonal of ***C***. Based on these decisions, the diagonal is decoded and fed back to remove the contribution of this diagonal from the received data. The receiver continues to decode the next diagonal and so on. The encoded substreams share a balanced presence over all paths to the receiver, so none of the individual substreams is subject to the worst path. Therefore, the data received at time t by the qth receive antenna is r_t^q, which contains a superposition of c_t^p, $p = 1, 2, \ldots, N_t$, and an AWGN noise component. Then, the received data vector can be expressed as $\mathbf{r}_t = \mathbf{H}_t \mathbf{c}_t + \xi_t$ at any time instance t. The D-BLAST method uses a repeated process of interference suppression, symbol detection, and interference

cancellation to decode all symbols, $c_t^{N_t}, c_t^{N_t-1}, ..., c_t^1$. This decoding process can be expressed in a general form described in the following.

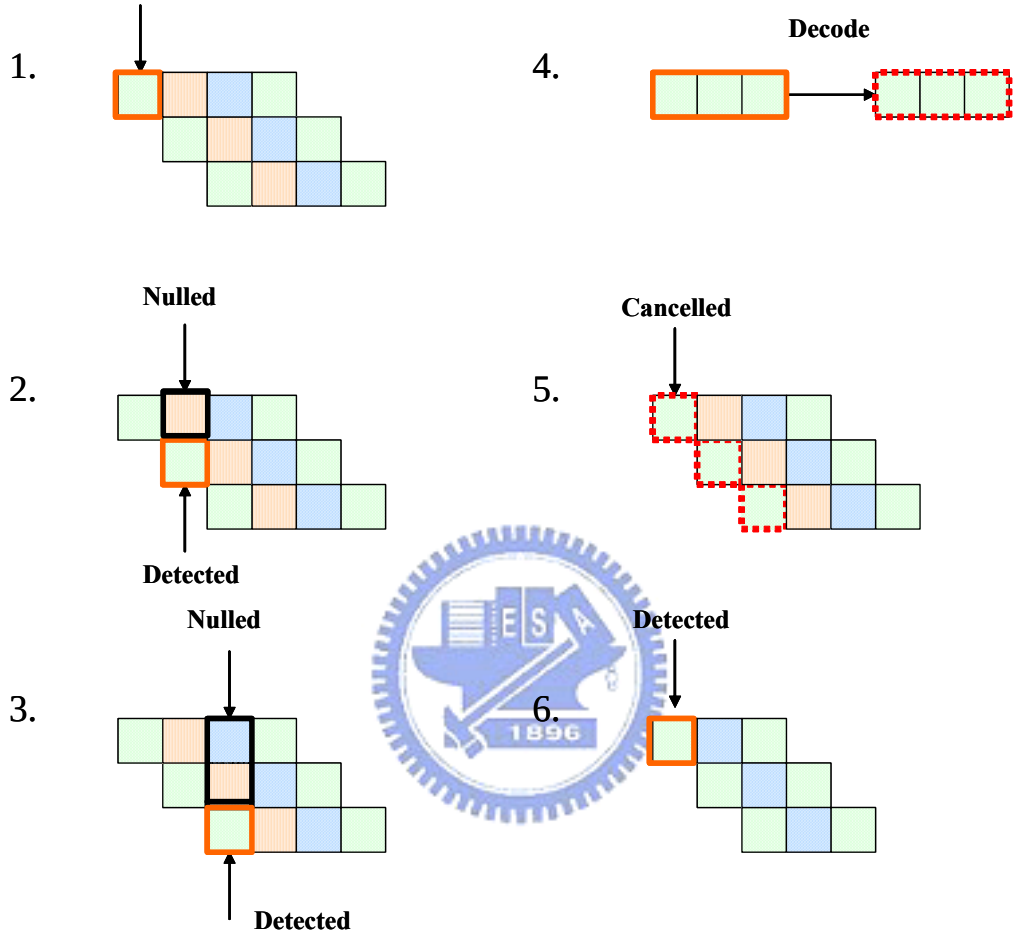

Figure 2.5: Diagonal Bell Labs' Layered Space-Time decoding procedure.

Let $\mathbf{Q}_t\mathbf{R}_t$ be the QR decomposition of $\mathbf{H}_t$, where $\mathbf{Q}_t$ is an $N_r \times N_r$ unitary matrix and $\mathbf{R}_t$ is an $N_r \times N_t$ upper triangular matrix. Multiplying the received signal by $\mathbf{Q}_t^H$, we can get

$$\begin{aligned}\mathbf{y}_t &= \mathbf{Q}_t^H\mathbf{r}_t = \mathbf{Q}_t^H\mathbf{H}_t\mathbf{c}_t + \mathbf{Q}_t^H\boldsymbol{\xi}_t = \underbrace{\mathbf{Q}_t^H\mathbf{Q}_t}_{\mathbf{I}_{N_r}}\mathbf{R}_t\mathbf{c}_t + \underbrace{\mathbf{Q}_t^H\boldsymbol{\xi}_t}_{\tilde{\boldsymbol{\xi}}_t} \\ &= \mathbf{R}_t\mathbf{c}_t + \tilde{\boldsymbol{\xi}}_t\end{aligned} \tag{2.36}$$

where

$$\mathbf{y}_t = \begin{bmatrix} y_t^1 \\ y_t^2 \\ \vdots \\ y_t^{N_r} \end{bmatrix}, \quad \mathbf{R}_t = \begin{bmatrix} r_t^{1,1} & r_t^{1,2} & \cdots & r_t^{1,N_t} \\ 0 & r_t^{2,2} & \cdots & r_t^{2,N_t} \\ 0 & 0 & \ddots & \vdots \\ \vdots & 0 & \ddots & r_t^{N_t,N_t} \\ 0 & \ddots & \ddots & 0 \\ 0 & 0 & \ddots & \vdots \\ 0 & 0 & \cdots & 0 \end{bmatrix}, \quad \tilde{\boldsymbol{\xi}}_t = \begin{bmatrix} \tilde{\xi}_t^1 \\ \tilde{\xi}_t^2 \\ \vdots \\ \tilde{\xi}_t^{N_r} \end{bmatrix} \tag{2.37}$$

Since $\mathbf{R}_t$ is a upper triangular matrix, the elements in the vector $\mathbf{y}_t$ can be expressed as

$$y_t^p = r_t^{p,p} c_t^p + \tilde{\xi}_t^p + \left\{\text{contribution from } c_t^{p+1}, c_t^{p+2}, ..., c_t^{N_t}\right\} \tag{2.38}$$

Hence, the interference from c_t^q, $q < p \le N_t$, is first suppressed in y_t^k and the residual interference terms in Equation (2.38) can be cancelled by the available decisions $\hat{c}_\tau^{p+1}, \hat{c}_\tau^{p+2}, \ldots, \hat{c}_\tau^{N_t}$. Assuming all these decisions are correct, then the present decision variable is

$$\tilde{c}_t^p = r_t^{p,p} c_t^p + \tilde{\xi}_t^p, \quad p = 1, 2, \ldots, N_t \tag{2.39}$$

The relation between c^p and $\tilde{c}^p$ in Equation (2.39) can be interpreted as the input and output of a SISO channel with the channel power gain $\left|r^{p,p}\right|^2$ and AWGN. The channel power gain $\left|r^{p,p}\right|^2$ is independently chi-squared distributed with $2\times(N_r-p+1)$ degrees of freedom. Moreover, if there are no decision feedback errors, the pth row of the $\boldsymbol{C}$ matrix can be treated as transmitted over a $(N_t, N_r)=(1, N_r-p+1)$ system without interference from the other rows and all fades are i.i.d.

2.4.2 Vertical Bell Lab's Layered Space-Time (V-BLAST)

The D-BLAST algorithm has been proposed by Foschini for achieving a substantial part of the MIMO capacity. In an independent Rayleigh scattering environment, this processing structure leads to theoretical rates which grow linearly with the number of antennas (assuming equal number of transmit and receive antennas) with these rates approaching ninety percents of Shannon capacity. However, the diagonal approach suffers from certain implementation complexities which make it inappropriate for practical implementation. Therefore, a simplified version of the BLAST algorithm is known as V-BLAST (vertical BLAST) [32], [33]. It is capable of achieving high spectral efficiency while being relatively simple to implement. The essential difference between D-BLAST and V-BLAST lies in the vector encoding process. In D-BLAST, redundancy between the substreams is introduced through the use of specialized intersubstream block coding. In V-BLAST, however, the vector encoding process is simply a demultiplex operation followed by independent bit-to-symbol mapping of each substream. No intersubstream coding, or coding of any kind, is required, though conventional coding of the individual substreams will certainly be applied.

Figure 2.6 shows the typical encoding steps in V-BLAST. The coding procedure can be viewed as there is an encoder on each transmit antenna. The output coded symbols of one encoder are transmitted from the corresponding transmit antenna. The output coded symbol of the *p*th encoder is used to fill the *p*th row of C.

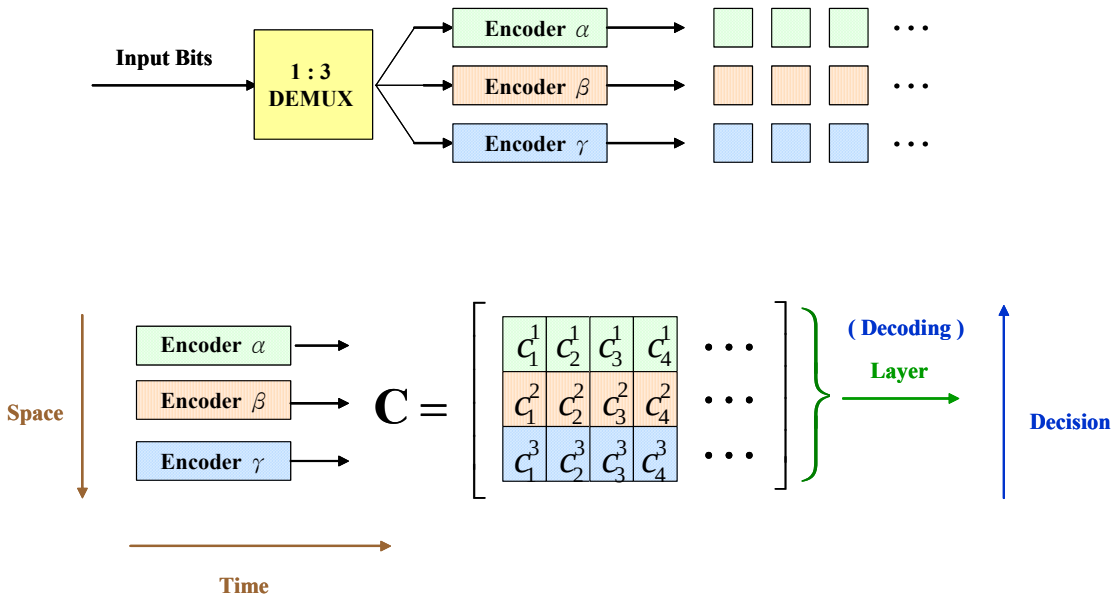

Figure 2.6: Vertical Bell Labs' Layered Space-Time encoding procedure.

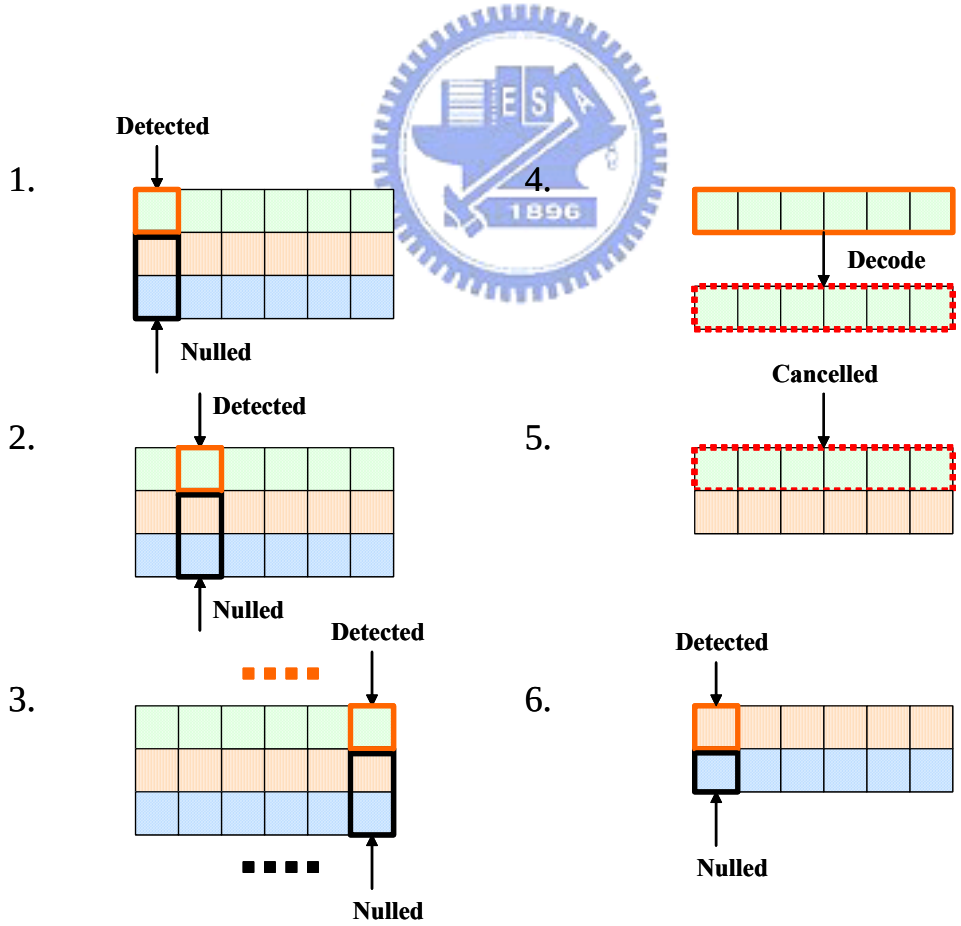

Figure 2.7: Vertical Bell Labs' Layered Space-Time decoding procedure.

Figure 2.7 shows the typical decoding steps in V-BLAST. The detection procedure is to extract the strongest substream from the signals received by the all receive antennas simultaneously. Then, the procedure proceeds with the remaining weaker signals, which are easier to recover when the strongest signals have been removed as a source of interference. Following the data model in D-BLAST, let $\tilde{\mathbf{H}}^{l=1} = \mathbf{H}_t$ and $\tilde{\mathbf{r}}^{l=1} = \mathbf{r}_t$ at the first decoding step at a given time instant t. In each step l, the pseudo-inverse of $\tilde{\mathbf{H}}^l$ is calculated to be the nulling matrix $\mathbf{G}^l$.

$$\begin{aligned} \mathbf{G}^l &= (\tilde{\mathbf{H}}^l)^+ \\ &= \left((\tilde{\mathbf{H}}^l)^H \tilde{\mathbf{H}}^l\right)^{-1} (\tilde{\mathbf{H}}^l)^H \end{aligned} \tag{2.40}$$

Each row of $\mathbf{G}^l$ can be used to null all but the lth desired signal. The layer shows the biggest post-processing SNR suggested to be detected first to reduce the error propagation effect efficiently [24]. At this step, the row of $\mathbf{G}^l$ with the minimum norm is chosen and the corresponding row is defined as the nulling vector $\mathbf{w}_{k_l}^T$.

$$k_l = \underset{j \notin \{k_1, \ldots, k_{l-1}\}}{\arg\min} \| (\mathbf{G}^l)_j \|^2 \tag{2.41}$$

$$\mathbf{w}_{k_l} = (\mathbf{G}^l)_{k_l}^T \tag{2.42}$$

The post-processing SNR for the k_lth detected component of **c** can be defined as

$$\rho_{k_l} = \frac{<| c^{k_l} |^2>}{\sigma^2 \| \mathbf{w}_{k_l} \|^2} \tag{2.43}$$

Then, using $\mathbf{w}_{k_l}$ to suppresses all layers but the one transmitted from antenna k_l and a soft decision value is obtained

$$\bar{c}_t^{k_l} = \mathbf{w}_{k_l}^T \tilde{\mathbf{r}}_t^l \tag{2.44}$$

Therefore, the k_l th layer can be detected within the constellation set S

$$\hat{c}_t^{k_l} = \underset{\tilde{x} \in S}{\arg\min} \| \tilde{c} - \bar{c}_t^{k_l} \|^2 \tag{2.45}$$

As soon as one layer is detected, the part of the detected signal can be subtracted from the received vector to improve the detection performance for the later layers.

$$\tilde{\mathbf{r}}_t^{l+1} = \tilde{\mathbf{r}}_t^{l} - \hat{c}_t^{k_l} \left(\tilde{\mathbf{H}}^{l}\right)^{k_l} \tag{2.46}$$

where $\left(\tilde{\mathbf{H}}^{l}\right)^{k_l}$ denotes the k_lth column of $\tilde{\mathbf{H}}^{l}$. Then, the channel matrix is deflated to account for its removal.

$$\tilde{\mathbf{H}}^{l+1} = \left(\tilde{\mathbf{H}}^{l}\right)^{\overline{k_l}} \tag{2.47}$$

where the notation $\left(\tilde{\mathbf{H}}^{l}\right)^{\overline{k_l}}$ denotes the matrix obtained by zeroing columns $k_1, k_2, ..., k_l$ of $\tilde{\mathbf{H}}^{l}$. Therefore, the diversity gain is increased by one at each step when we decrease the number of layers to be nulled out in the next step by one.

The Zero-Forcing (ZF) V-BLAST detection algorithm can be summarized as follows:

Initialization:

$i \leftarrow 1$

$\mathbf{G}^1 = \left(\tilde{\mathbf{H}}^1\right)^{+}$

$k_1 = \arg\min_j \| (\mathbf{G}^1)_j \|^2$

Recursion:

$\mathbf{w}_{k_l} = (\mathbf{G}^l)_{k_l}^T$

$\overline{c}^{k_l} = \mathbf{w}_{k_l}^T \tilde{\mathbf{r}}^l$

$\overline{c}^{k_l} = \mathbf{w}_{k_l}^T \tilde{\mathbf{r}}^l$

$\hat{c}^{k_l} = Q(\overline{c}^{k_l})$

$\mathbf{r}^{l+1} = \mathbf{r}^l - \hat{c}^{k_l} (\tilde{\mathbf{H}}^l)^{k_l}$

$\tilde{\mathbf{H}}^{l+1} = \left(\tilde{\mathbf{H}}^{l}\right)^{\overline{k_l}}$

$\mathbf{G}^{l+1} = \left(\tilde{\mathbf{H}}^{l+1}\right)^{+}$

$k_{l+1} = \arg \min_{j \notin \{k_1, \cdots k_l\}} \| (\mathbf{G}^{l+1})_j \|^2$

$i \leftarrow i + 1$

By using the minimum mean square error (MMSE) nulling matrix instead of the ZF one, it can improve the detection performance especially for the mid-range SNR values [32].

$$\mathbf{G}^{l} = \left((\tilde{\mathbf{H}}^{l})^{H} \tilde{\mathbf{H}}^{l} + \frac{1}{SNR} \mathbf{I} \right)^{-1} (\tilde{\mathbf{H}}^{l})^{H} \tag{2.48}$$

In the MMSE detection case, the noise level on the channel is taken into account besides nulling out the interference. Thus, the SNR has to be estimated at the receiver

2.5 Beamforming Based on MIMO Techniques

Traditionally, the intelligence of the multiantenna system is located in the weight selection algorithm. Simple linear combining can offer a more reliable communications link in the presence of adverse propagation conditions such as multipath fading and interference. Beamforming is a key technique in smart antenna and increases the average SNR. In the following, we will introduce two schemes: beamforming and eigenbeamforming.

2.5.1 Generic Beamforming

As a feedback channel from the receiver to the transmitter can be obtained, beamforming can be utilized to maximize the receiver SNR and provide array gain [33]. With beamforming technique applied to both transmitter and receiver, the beamformer output of the receiver is given by

$$\hat{s} = \mathbf{w}_{R}^{H} \left(\mathbf{H} \mathbf{w}_{T} s + \mathbf{n} \right) = \mathbf{w}_{R}^{H} \mathbf{H} \mathbf{w}_{T} s + \mathbf{w}_{R}^{H} \mathbf{n} \tag{2.49}$$

where $\mathbf{w}_R$ and $\mathbf{w}_T$ denote the weight vectors of transmitter and receiver, respectively, $\mathbf{x} = \mathbf{w}_T s$ is the transmitted signal vector, and $\mathbf{n}$ is Gaussian noise. If $\mathbf{w}_R$ and $\mathbf{w}_T$ are chosen as the dominant left and right singular vectors associated with the channel

matrix **H**, the beamformer output can be rewritten as

$$\hat{s} = \lambda_1^{1/2} s + \mathbf{w}_R^* \mathbf{n} \tag{2.50}$$

where λ_1 is the largest eigenvalue of the matrix $\mathbf{H}\mathbf{H}^H$. According to Equation (2.50), the corresponding SNR is

$$\mathrm{SNR}_{\mathrm{BF}} = \frac{P_T}{\sigma_n^2} \lambda_1 \tag{2.51}$$

where P_T is the total transmitted power.

2.5.2 Eigenbeamforming Technique

The eigenbeamforming is an attractive method for downlink [34]. It can provide good diversity gains with less amount of feedbacks due to the short-term selection of eigenmode. Eigenbeamforming is particularly suitable for spatially correlation channels, and is easily applied to the spatial downlink channel. This is because that the spatial downlink channel possesses a higher spatial correlation and few dominant eigenmodes, in which each eigenmode can be considered as an uncorrelated path to the mobile station [35]. In a cellular system, the signal can be spatially selectively transmitted with only few directions due to the vanish of local scatters around the antenna array of the base station. This makes the eigenbeamforming effectively. Consider a system with N_T transmit antennas at the base station and N_R receive antennas at the mobile station. The received signal vector at the mobile station is given by

$$\mathbf{y}(t) = \sqrt{\gamma}\mathbf{H}(t)\mathbf{w}(t)s(t) + \mathbf{n}(t) \tag{2.52}$$

where γ is the input SNR, **H**(*t*) is the channel matrix, and **w**(*t*) is the beamforming weight vector. Assume that beamforming vector is normalized to one, i.e., $\|\mathbf{w}(t)\|^2 = 1$.

The instantaneous SNR at the receiver is written as

$$\gamma_{rec} = \gamma \mathbf{w}^H(t)\mathbf{H}^H(t)\mathbf{H}(t)\mathbf{w}(t) \tag{2.53}$$

This suggests that the optimal weight vector, maximizing the instantaneous SNR, can be obtained as follows:

$$\mathbf{w}_{opt}(t) = \arg\max_{\|\mathbf{w}\|^2=1} \mathbf{w}^H(t)\mathbf{R}_{\mathbf{H}}(t)\mathbf{w}(t) \tag{2.54}$$

where $\mathbf{R}_{\mathbf{H}}(t) = \mathbf{H}^H(t)\mathbf{H}(t)$. The corresponding solution is the dominant eigenvector associated with the largest eigenvalue of the matrix $\mathbf{R_H}(t)$. Note that since the channel information must be sent to the base station, this method is called close-loop beamforming. Suppose that the instantaneous channel matrix is not available. Assume that the beamforming vector is time-invariant (or very slowly varying). The beamforming vector can be obtained by maximizing the mean SNR as follows:

$$\begin{aligned}\mathbf{w}_{ms} &= \arg\max_{\|\mathbf{w}\|^2\le 1} E\left[\gamma_{rec}(t)\right] \\ &= \arg\max_{\|\mathbf{w}\|^2\le 1} \mathbf{w}^H\mathbf{R}_{\mathbf{H}}\mathbf{w}\end{aligned} \tag{2.55}$$

where $\mathbf{R}_{\mathbf{H}} = E\left[\mathbf{R}_{\mathbf{H}}(t)\right]$. The beamforming that uses $\mathbf{w}_{ms}$ is called the blind beamforming that can be employed in CDMA system with lower mobile speed.

2.6 Review of OFDM

OFDM is a special case of multicarrier transmission, where a single data stream is transmitted over a number of low data rate subcarriers. OFDM can be thought of as a hybrid of multicarrier modulation (MCM) and frequency shift keying (FSK) modulation scheme. The principle of MCM is to transmit data by dividing the data stream into several parallel data streams and modulate each of these data streams onto individual subcarriers. FSK modulation is a technique whereby data is transmitted on one subcarrier from a set of orthogonal subcarriers in symbol duration. Orthogonality

between these subcarriers is achieved by separating these subcarriers by an integer multiples of the inverse of symbol duration of the parallel data streams. With the OFDM technique used, all orthogonal subcarriers are transmitted simultaneously. In other words, the entire allocated channel is occupied through the aggregated sum of the narrow orthogonal subbands.

The main reason to use OFDM systems is to increase the robustness against frequency-selective fading or narrowband interference. In a single carrier system, a single fade or interference can cause the entire link fail, but in a multicarrier system, only a small amount of subcarriers will be affected. Then the error correction coding techniques can be used to correct errors. The equivalent complex baseband OFDM signal can be expressed as

$$x(t)=\begin{cases}\sum_{k=-\frac{N_c}{2}}^{\frac{N_c}{2}-1} d_k\phi_k(t) & 0\le t\le T\\ 0 & \text{Otherwise}\end{cases}=\left[\sum_{k=-\frac{N_c}{2}}^{\frac{N_c}{2}-1} d_k\phi_k(t)\right]u_T(t) \tag{2.56}$$

where N_c is the number of subcarriers, T is the symbol duration, d_k is the transmitted subsymbol (M-PSK or M-QAM), $\phi_k(t)=e^{j2\pi f_k t}/\sqrt{T}$ is the kth subcarrier with the frequency $f_k=k/T$, and $u_T(t)$ is the time windowing function. Using the correlator-based OFDM demodulator, the output of the jth branch can be presented as

$$\begin{aligned} y_j &= \int_0^T x(t)\phi_j^*(t)dt = \frac{1}{T}\sum_{k=-\frac{N_c}{2}}^{\frac{N_c}{2}-1} d_k\int_0^T e^{j2\pi\frac{k-j}{T}t}dt \\ &= d_j \end{aligned} \tag{2.57}$$

By sampling $x(t)$ with the sampling period $T_d=T/N_c$, the discrete time signal x_n can be expressed as

$$x_n = x(t)\big|_{t=nT_d} = \begin{cases} \dfrac{1}{\sqrt{N_c}} \displaystyle\sum_{k=-\frac{N_c}{2}}^{\frac{N_c}{2}-1} d_k e^{j2\pi\frac{k}{N_c}n} & 0 \le n \le N_c - 1 \\ 0 & \text{Otherwise} \end{cases} = \text{IFFT}\{d_k\} \tag{2.58}$$

Note that x_n is the inverse fast Fourier transform (IFFT) output of the N input data subsymbols. Similarly, the output of the jth branch can also be presented in the digital form

$$y_j = \text{FFT}\{x_n\} = \frac{1}{\sqrt{N_c}} \sum_{n=0}^{N_c-1} x_k e^{-j2\pi\frac{j}{N_c}n} = \sum_{k=-\frac{N_c}{2}}^{\frac{N_c}{2}-1} x_k \delta[k-j] = d_j \tag{2.59}$$

In theory, the orthogonality of subcarriers in OFDM systems can be maintained and individual subcarriers can be completely separated by the fast Fourier transform (FFT) at the receiver when there are no intersymbol interference (ISI) and intercarrier interference (ICI) introduced by transmission channel distortions. However, it is impossible to obtain these conditions in practice. In order to eliminate ISI completely, a guard interval is imposed into each OFDM symbol. The guard interval is chosen larger than the expected delay spread, such that the multipath from one symbol cannot interfere with the next symbol as shown in Figure 2.8. The guard interval can consist of no signals at all. However, the effect of ICI would arise in that case due to the loss of orthogonality between subcarriers. To eliminate ICI, the OFDM symbol is cyclically extended in the guard interval to introduce cyclic prefix (CP) as shown in Figure 2.9. This ensures that delayed replicas of the OFDM symbol always have an integer number of cycles within the FFT interval, as long as the delay is smaller than the guard interval. As a result, the delayed multipath signals which are smaller than the guard interval will not cause ICI.

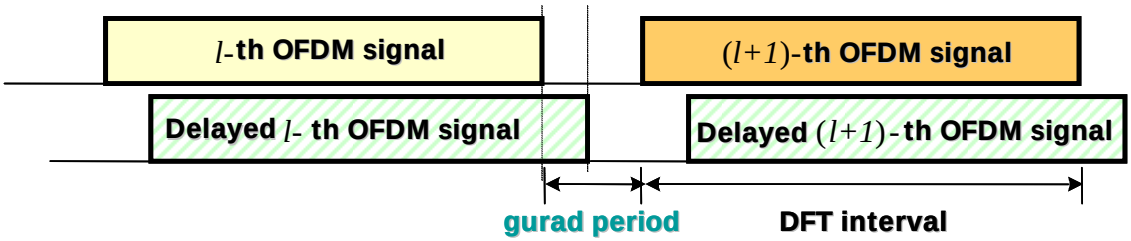

Figure 2.8: The effect of guard period in multipath case

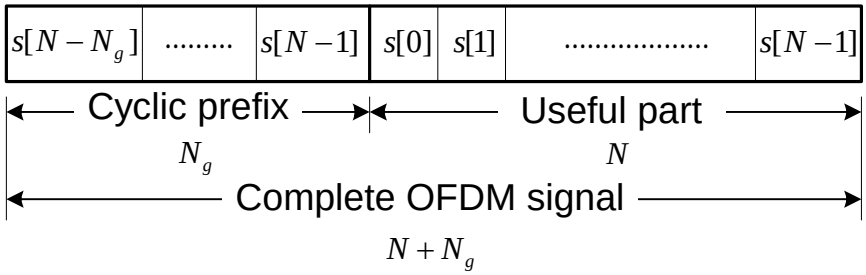

Figure 2.9: Structure of complete OFDM signal with guard period

The complete OFDM signal with CP is given by

$$\tilde{x}_n = \begin{cases} \dfrac{1}{\sqrt{N_c}} \displaystyle\sum_{k=-\frac{N_c}{2}}^{\frac{N_c}{2}-1} d_k e^{j2\pi \frac{k}{N_c}(n-N_{cp})} & 0 \le n \le N_c + N_{cp} - 1 \\ 0 & \text{Otherwise} \end{cases} \tag{2.60}$$

where N_{cp} is the number of samples in CP. Due to CP, the transmitted OFDM symbol becomes periodic, and the linear convolution process of the transmitted OFDM symbols with the channel impulse responses will become a circular convolution one. Assuming the value of N_{cp} is larger than the channel length, the received data vector can be expressed as

$$\mathbf{y} = \mathbf{H}\mathbf{x} + \boldsymbol{\eta} \tag{2.61}$$

$$\underbrace{\begin{bmatrix} y_{N_c-1} \\ \vdots \\ y_0 \end{bmatrix}}_{\mathbf{y}} = \underbrace{\begin{bmatrix} h_0 & h_1 & \cdots & h_{N_{cp}} & 0 & \cdots & 0 \\ 0 & h_0 & h_1 & \cdots & h_{N_{cp}} & 0 & \vdots \\ 0 & 0 & \ddots & \ddots & \cdots & \ddots & 0 \\ 0 & \cdots & 0 & h_0 & h_1 & \cdots & h_{N_{cp}} \end{bmatrix}}_{\mathbf{H}} \underbrace{\begin{bmatrix} x_{N_c-1} \\ \vdots \\ x_0 \\ x_{-1} \\ \vdots \\ x_{-N_{cp}} \end{bmatrix}}_{\mathbf{x}} + \underbrace{\begin{bmatrix} \eta_{N_c-1} \\ \vdots \\ \eta_0 \end{bmatrix}}_{\boldsymbol{\eta}} \tag{2.62}$$

Applying SVD on the channel response, we have

$$\mathbf{H} = \mathbf{U}\boldsymbol{\Sigma}\mathbf{V}^H \tag{2.63}$$

where $\mathbf{U}$ and $\mathbf{V}$ are unitary matrices, and $\boldsymbol{\Sigma}$ is a diagonal matrix. Substituting Equation (2.63) and the equalities of $\mathbf{x} = \mathrm{V}\mathbf{X}$ and $\mathbf{Y} = \mathrm{U}^H\mathbf{y}$ into Equation (2.62), the received data vector can be written as

$$\mathbf{Y} = \mathbf{U}^H\mathbf{y} = \mathbf{U}^H(\mathbf{H}\mathbf{x} + \boldsymbol{\eta}) = \mathbf{U}^H\mathbf{H}\mathbf{V}\mathbf{X} + \underbrace{\mathbf{N}}_{\mathbf{U}^H\boldsymbol{\eta}} = \boldsymbol{\Sigma}\mathbf{X} + \mathbf{N} \tag{2.64}$$

This means that the output $\mathbf{Y}$ can be expressed in terms of the product of $\boldsymbol{\Sigma}$ and $\mathbf{X}$ plus noise. When $x_{-i} = x_{N-i}$ for $i = 1, \ldots, N_{cp}$, a more compact matrix form of the guard interval can be written as

$$\begin{bmatrix} y_{N_c-1} \\ \vdots \\ y_0 \end{bmatrix} = \begin{bmatrix} h_0 & h_1 & \cdots & h_{N_{cp}} & 0 & \cdots & 0 \\ 0 & h_0 & h_1 & \cdots & h_{N_{cp}} & \ddots & 0 \\ \vdots & \ddots & \ddots & \ddots & \ddots & \ddots & \vdots \\ 0 & \cdots & 0 & h_0 & h_1 & \cdots & h_{N_{cp}} \\ h_{N_{cp}} & 0 & \cdots & 0 & h_0 & \cdots & h_{N_{cp}-1} \\ \vdots & \ddots & \ddots & \ddots & \ddots & \ddots & \vdots \\ h_1 & \cdots & h_{N_{cp}} & 0 & \cdots & 0 & h_0 \end{bmatrix} \begin{bmatrix} x_{N_c-1} \\ \vdots \\ x_0 \end{bmatrix} + \begin{bmatrix} \eta_{N_c-1} \\ \vdots \\ \eta_0 \end{bmatrix} \tag{2.65}$$

where $\mathbf{H}$ becomes a circulant matrix ($\mathbf{H} = \mathbf{Q}^H\boldsymbol{\Lambda}\mathbf{Q}$) and $\mathbf{Q}$ is a discrete Fourier transform (DFT) matrix with the lth entry as

$$\mathbf{Q}_l = \frac{1}{\sqrt{N_c}} e^{-j2\pi\frac{l}{N_c}} \tag{2.66}$$

As shown in Equation (2.64), the received data $\mathbf{y}$ can be transformed into $\mathbf{Y}$

$$\mathbf{Y} = \mathbf{Q}^H \mathbf{y} = \mathbf{Q}^H (\mathbf{H}\mathbf{x} + \boldsymbol{\eta}) = \underbrace{\mathbf{Q}^H \mathbf{H} \mathbf{Q}^H}_{\boldsymbol{\Sigma}} \mathbf{X} + \underbrace{\mathbf{Q}^H \boldsymbol{\eta}}_{\mathbf{N}} \tag{2.67}$$
$$= \boldsymbol{\Sigma}\mathbf{X} + \mathbf{N}$$

According to Equation (2.67), by adding CP to the OFDM symbol, the modulation in OFDM is equivalent to multiplying the frequency domain signals of the OFDM symbol with the channel's frequency response $\boldsymbol{\Sigma}$.

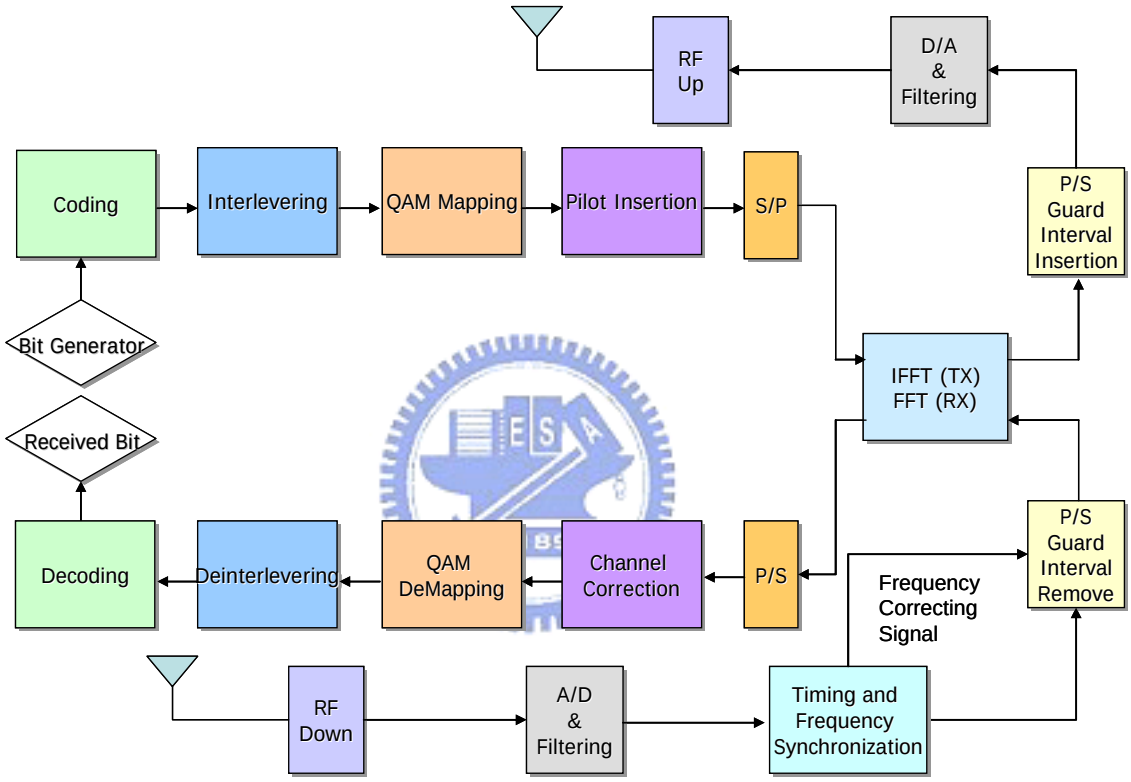

Figure 2.10: Transceiver for OFDM systems

The block diagrams of the OFDM transceiver is shown in Figure 2.10, where the upper path is the transmitter chain and lower path corresponds to the receiver chain. In the center, IFFT modulates a block of input values onto a number of subcarriers. In the receiver, the subcarriers are demodulated by the FFT, which performs the reverse operation of the IFFT. In fact, the IFFT can be made using the FFT by conjugating input and output of the FFT and dividing the output by the FFT size. This makes it

possible to use the same hardware for both transmitter and receiver. This complexity saving is only possible when the transceiver doesn't have to transmit and receive simultaneously. The functions before the IFFT can be discussed as follows. Binary input data is first encoded by a forward error correction code. The encoded data is then interleaved and mapped onto QAM values. In the receiver path, after passing the radio frequency (RF) part and the analog-to-digital conversion (ADC), the digital signal processing starts with a training sequence to determine symbol timing and frequency offset. The FFT is used to demodulate all subcarriers. The FFT outputs are mapped onto binary values and decoded to produce binary output data. In order to successfully map the QAM values onto binary values, the reference phases and amplitudes of all subcarriers have to be acquired first.

In conclusion, OFDM is a powerful modulation technique that simplifies the removal of distortion due to the multipath channel and increases bandwidth efficiency. The key advantages of OFDM transmission scheme can be summarized as follows:

1. OFDM is an efficient way to deal with multipath. For a given delay spread, the implementation complexity is significantly lower than that of a single carrier system with an equalizer.
2. In relatively slow time-varying channels, it is possible to significantly enhance the capacity by adapting the data rate per subcarrier according to the signal-to-noise ratio (SNR) of that particular subcarrier.
3. OFDM is robust against narrowband interference because such interference affects only a small amount of subcarriers.
4. OFDM makes single-frequency networks possible, which is especially attractive for broadcasting applications.

2.7 Summary

Information theory shows that MIMO communication systems can significantly increase the capacity of band-limited wireless channels by a factor of the minimum number of transmit and receive antennas, provided that a rich multipath scattering environment is considered. In Sections 2.2 MIMO system model and MIMO channel capacity are introduced.

New degrees of freedom in spatial domain provided by multiple antennas are introduced in Section 2.3. The diversity makes us choose the better subchannel to transmit data which increasing the system performance in BER curve.

In order to achieve a high data rate in MIMO systems, spatial multiplexing technique is presented in Section 2.4. Spatial multiplexing allows significant data rate enhancement in a wireless radio link without additional power or bandwidth consumption. It is realized by transmitting independent data signals from the individual transmit antennas. Two typical spatial multiplexing schemes, D-BLAST and V-BLAST, are introduced in Sections 2.4.1 and 2.4.2.

Another technique called beamforming is described in Section 2.5. Beamforming is implemented by multiplying the symbol(s) with appropriate beamforming vactor(s) both at the transmitter and the receiver. While CSI is available both at the transmitter and the receiver, MIMO systems can benefit from significant diversity and codign gains by using beamforming.

OFDM has gained wide acceptance in wireless communications as an appropriate broadband modulation scheme. OFDM systems have the desirable immunity to intersymbol interference (ISI) caused by the delay spread of wireless channels. Therefore, it is a promising technique for high data rate transmission over frequency-selective fading channels. In Section 2.6, OFDM systems are introduced.

Chapter 3

Joint Beamforming and Subcarrier Allocation for Multiuser MIMO-OFDM Systems

Multiple-input multiple-output (MIMO) systems where multiple antennas are used at both the transmitter and receiver have been acknowledged as one of the most promising techniques to achieve dramatic improvement in physical-layer performance. Moreover the use of multiple antennas enables space-division multiple access (SDMA), which allows intracell bandwidth reuse by multiplexing spatially separable users [36], [37]. Channel variation in the spatial domain also provides an inherent DOF (Degree of Freedom) for adaptive transmissions. Recently, multiuser adaptive transmission in multiple-antenna systems has been reported in [38] and [39] to exploit the space and multiuser diversity from an information theory point of view.

In Chapter 3, we will propose two algorithms: the first one is to design transmit and receive beamforming in order to cancel interference between users in downlink case and use SVD (Singular Value Decomposition) decomposition to simplify the design procedure and ensure good performance. The second method is to select N users transmitting data on the same subcarrier where N is the number of transmit and receive antennas. With this method, we can execute the subcarrier allocation process.

This chapter is organized as follows. First, SVD decomposition is introduced whose mathematical form and physical meaning will be given. Second, we formulate the problem of beamforming design and show how to find the beamformer with SVD. Finally, we propose a method of allocating subcarriers to maximize the system transmission rate and show the simulation results of above algorithms.

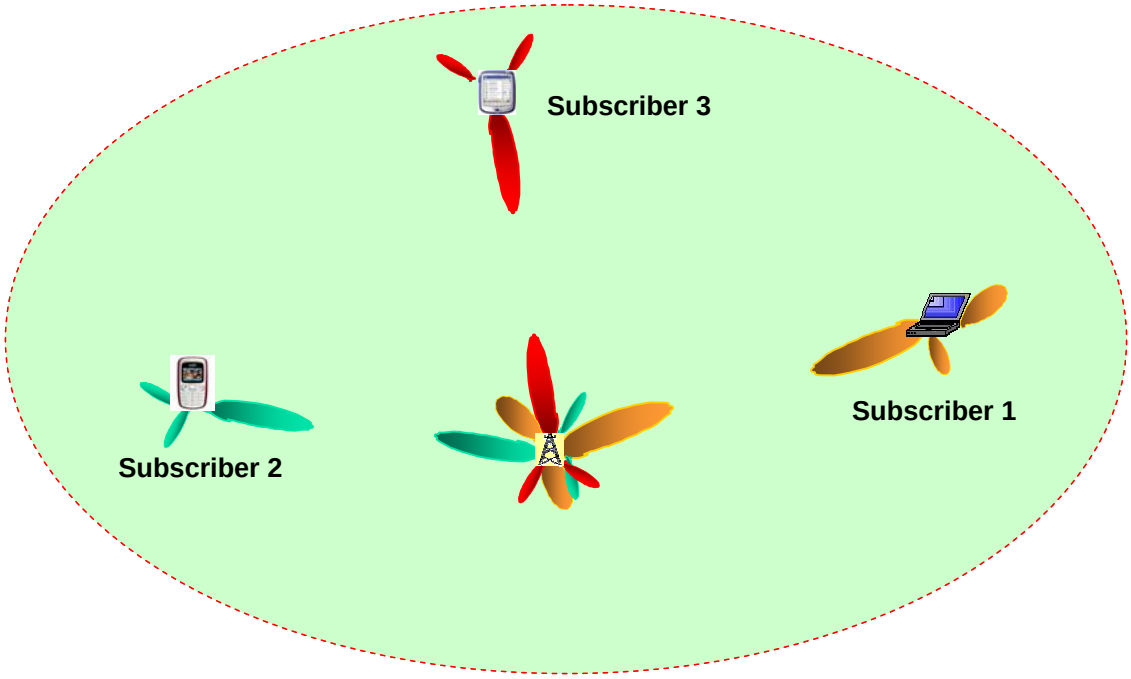

Figure 3.1: Scenario of transmit and receive beamformer to null interference

3.1 System Model and Problem Formulation

In multiuser systems, interference is the most important factor that dominates the system performance. Consequently, we try to design the transmit and receive beamformer in downlink case for interference cancellation. The algorithm is SVD based because it can simplify the design. The scenario is shown in Figure 3.1.

3.1.1 Singular Value Decomposition (SVD)

From basic linear algebra, every linear transformation can be represented as a composition of three operations: a rotation operation, a scaling operation, and another rotation operation. In the notation of matrices, the matrix **H** has a singular value decomposition (SVD):

$$\mathbf{H} = \mathbf{U}\mathbf{\Lambda}\mathbf{V}^{*} \quad , \forall \mathbf{H} \in \mathrm{C}^{M \times N}, \tag{3.1}$$

where $\mathbf{U} \in C^{M \times M}$ and $\mathbf{V} \in C^{N \times N}$ are unitary matrix, $\mathbf{\Lambda} \in R^{M \times N}$ is diagonal matrix whose diagonal elements are nonnegative real numbers and whose off-diagonal elements are zero. The diagonal elements $\lambda_1 \geq \lambda_2 \geq ... \geq \lambda_{N_{\min}}$ are the ordered singular values of the matrix **H**, where $N_{\min} \triangleq \min(M, N)$. We can rewrite the SVD as

$$\mathbf{H} = \sum_{i}^{N_{\min}} \lambda_i \mathbf{u}_i \mathbf{v}_i^{*} \tag{3.2}$$

i.e., the sum of rank-one matrices $\lambda_i \mathbf{u}_i \mathbf{v}_i^{*}$'s. It can be seen that the rank of **H** is precisely the number of non-zero singular values.

The SVD decomposition can be interpreted as two coordinate transformations: it says that if the input is expressed in terms of a coordinate system defined by the columns of **V** and the output is expressed in terms of a coordinate system defined by the columns of **U**, then the input-output relationship is very simple. The equivalence is summarized in Figure 3.2

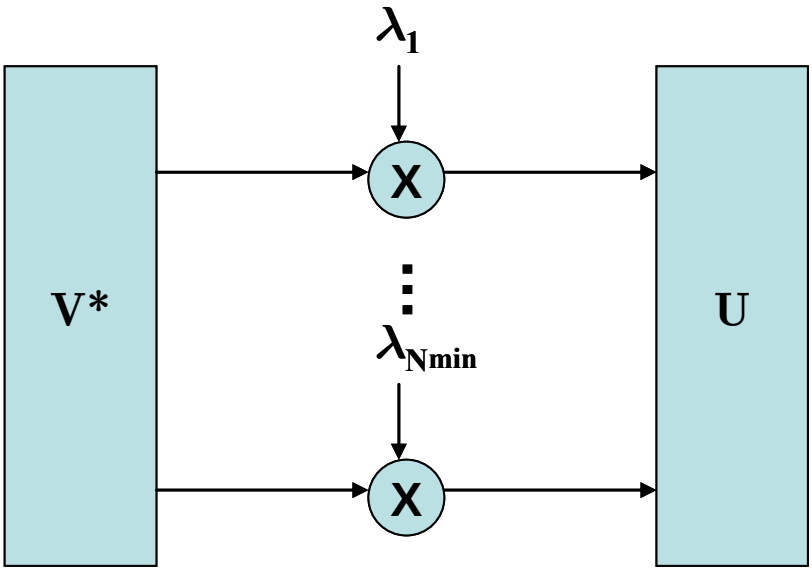

Figure 3.2: Converting **H** into a parallel channel through the SVD

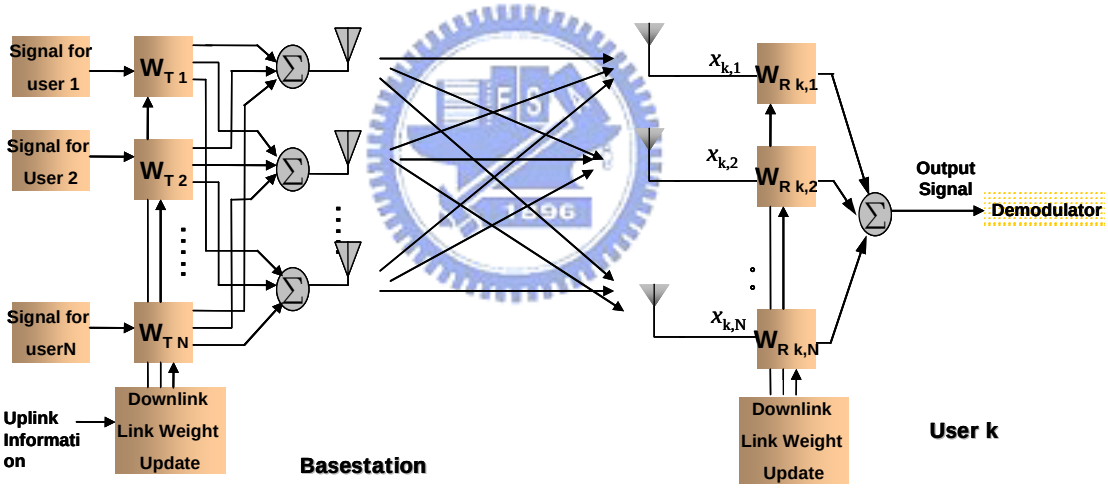

Figure 3.3: Block diagram of proposed MIMO-OFDM system with adaptive beamforming

3.1.2 System Model

The system under consideration is given in Figure 3.3. We consider the downlink case. For each user *k* we want to design the transmit beamformer $\mathbf{w}_{T_k}$ and receive beamformer $\mathbf{w}_{R_k}$ to null the interference between users occupying the same subcarrier.

We assume that each user and base station are equipped with *N* antennas.

We consider the downlink case. There are *N* subscribers in one cell. The signal transmitted for user k is S_k. w_{T_k} and $\mathbf{w}_{R_k}$ represent the transmit and receive beamforming vector of user *k*. The total transmit signal after beamforming can be written as

$$S_{trans} = \sum_{i=1}^{N} \mathbf{W}_{\mathbf{T}_i} S_i \,. \tag{3.3}$$

If the length of the cyclic prefix is longer than the maximum time dispersion of the channel response, then the channel appears to be flat on each subcarrier. Denote the channel matrix of user *k* by

$$\mathbf{H}_k = \begin{bmatrix} h_{1,1}^k & h_{1,2}^k & \cdots & h_{1,N}^k \\ h_{2,1}^k & h_{2,2}^k & \cdots & h_{2,N}^k \\ \vdots & \vdots & \ddots & \vdots \\ h_{N,1}^k & h_{N,2}^k & \cdots & h_{N,N}^k \end{bmatrix} \tag{3.4}$$

where $h_{i,j}^k$ is the channel gain from the *j*th transmit antenna to the *l*th receive antenna. The signal received at user *k* is

$$\mathrm{S}_{\mathrm{re}_k} = \mathbf{H}_k \cdot \left(\sum_{i=1}^{N} \mathbf{W}_{\mathbf{T}_i} S_i \right) + \mathbf{n}_k \tag{3.5}$$

After receive beamforming, the signal received at user *k* becomes

$$\mathbf{w}_{\mathbf{R}_k}^{\mathrm{H}} \left(\mathbf{H}_k \cdot \left(\sum_{i=1}^{N} \mathbf{w}_{\mathbf{T}_i} S_i \right) + \mathbf{n}_k \right) \tag{3.6}$$

3.2 Proposed Beamforming Scheme with Interference Nulling

In ZF algorithm, we hope that the gain of desired signal is normalized to 1 and the gain of the interference is zero. This concept can be written as matrix form as follows:

$$\begin{bmatrix} \mathbf{w}_{R_1}^H \mathbf{H}_1 \mathbf{w}_{T_1} & \mathbf{w}_{R_1}^H \mathbf{H}_1 \mathbf{w}_{T_2} & \cdots & \mathbf{w}_{R_1}^H \mathbf{H}_1 \mathbf{w}_{T_N} \\ \mathbf{w}_{R_2}^H \mathbf{H}_2 \mathbf{w}_{T_1} & \mathbf{w}_{R_2}^H \mathbf{H}_2 \mathbf{w}_{T_2} & \cdots & \mathbf{w}_{R_2}^H \mathbf{H}_2 \mathbf{w}_{T_N} \\ & \vdots & & \\ \mathbf{w}_{R_N}^H \mathbf{H}_N \mathbf{w}_{T_1} & \mathbf{w}_{R_N}^H \mathbf{H}_N \mathbf{w}_{T_2} & \cdots & \mathbf{w}_{R_N}^H \mathbf{H}_N \mathbf{w}_{T_N} \end{bmatrix} = \mathbf{I}_{N\times N}, \tag{3.7}$$

where the (m,n)th element of matrix is the gain of signal n received by user m. The above matrix equation can be decomposed and the right identity matrix can be viewed as a diagonal matrix in general form. In this reason, we rewrite the equation as

$$\begin{bmatrix} \mathbf{w}_{R_1}^H & \mathbf{0}^H & \cdots & \mathbf{0}^H \\ \mathbf{0}^H & \mathbf{w}_{R_2}^H & \cdots & \mathbf{0}^H \\ \vdots & \vdots & \ddots & \vdots \\ \mathbf{0}^H & \mathbf{0}^H & \cdots & \mathbf{w}_{R_N}^H \end{bmatrix}_{N\times N^2} \begin{bmatrix} \mathbf{H}_1 \\ \mathbf{H}_2 \\ \vdots \\ \mathbf{H}_N \end{bmatrix}_{N^2\times N} \begin{bmatrix} \mathbf{w}_{T_1} & \mathbf{w}_{T_2} & \cdots & \mathbf{w}_{T_N} \end{bmatrix}_{N\times N} = \Lambda_{N\times N} \tag{3.8}$$

Define $\mathbf{H}_{N^2\times N} = [\mathbf{H}_1{}^H, \mathbf{H}_2{}^H, ..., \mathbf{H}_N{}^H]^H$. Using SVD decomposition, we can get

$$\mathbf{H} = \sum_{i=1}^{N} \mathbf{u}_i \alpha_i \mathbf{v}_i^H \tag{3.9}$$

Let transmit beamformer be right singular vector of $\mathbf{H}$ (ex: $\mathbf{w}_{T_i} = \mathbf{v}_i$). Therefore the equation (3.9) becomes

$$\begin{bmatrix} \alpha_1 \mathbf{w}_{R_1}^H \mathbf{u}_1(1:N) & \alpha_2 \mathbf{w}_{R_1}^H \mathbf{u}_2(1:N) & \cdots & \alpha_N \mathbf{w}_{R_1}^H \mathbf{u}_N(1:N) \\ \alpha_1 \mathbf{w}_{R_2}^H \mathbf{u}_1(N+1:2N) & \alpha_2 \mathbf{w}_{R_2}^H \mathbf{u}_2(N+1:2N) & \cdots & \alpha_N \mathbf{w}_{R_2}^H \mathbf{u}_N(N+1:2N) \\ \vdots & \vdots & \ddots & \vdots \\ \alpha_1 \mathbf{w}_{R_N}^H \mathbf{u}_1(N(N-1)+1:N^2) & \alpha_2 \mathbf{w}_{R_N}^H \mathbf{u}_2(N(N-1)+1:N^2) & \cdots & \alpha_N \mathbf{w}_{R_N}^H \mathbf{u}_N(N(N-1)+1:N^2) \end{bmatrix}_{N\times N} = \Lambda_{N\times N} \tag{3.10}$$

Now, we want to find a set of vectors $\{\mathbf{w}_{R_k}\}, \forall k \in \{1,...,N\}$ to satisfy the above equation. One possible solution can be find by satisfying the equation

$$\mathbf{w}_{R_k}^H \times [\mathbf{u}_1(N(k-1)+1:Nk) \quad \mathbf{u}_2(N(k-1)+1:Nk) \quad \cdots \quad \mathbf{u}_N(N(k-1)+1:Nk)] = e_k^T \tag{3.11}$$

Consequently

$$\mathbf{w}_{R_k}^H = \left[\mathbf{e}_k^T \cdot \mathbf{u}_k^{-1} \right] \tag{3.12}$$

where

$$\mathbf{u}_k \triangleq [\mathbf{u}_1(N(k-1)+1:Nk) \quad \mathbf{u}_2(N(k-1)+1:Nk) \quad \cdots \quad \mathbf{u}_N(N(k-1)+1:Nk)]. \tag{3.13}$$

The SNR_k after beamforming is given by

$$\text{SNR}_k = \alpha_k^2 / (\left\| \mathbf{w}_{T_k} \right\|^2 \sigma_n^2) \tag{3.14}$$

3.3 Computer Simulations of ZF Algorithm

Before giving the simulation results, we define the relation between SNR and E_b/N_0 at each receive antenna as follows:

$$\text{SNR} = \frac{\text{signal power}}{\text{noise power}} = \frac{\frac{E_s}{T_s}}{N_0 B} = \frac{\frac{E_b \cdot N_t \cdot M}{T_s}}{N_0 \frac{1}{T_s}} = \frac{E_b}{N_0} \cdot (N_t \cdot M) \tag{3.15}$$

where E_s is the symbol energy, T_s is the symbol duration, B is the system bandwidth and M is the modulation order. Throughout the following simulations, the system transmit power is normalized to 1, and hence the noise power corresponding to a specific E_b/N_0 is generated by

$$\text{noise power} = \frac{N_0}{E_b \cdot N_t \cdot M}. \tag{3.16}$$

This result is utilized in the following of this thesis.

The parameter of simulation is shown in Table 3.1. Here we assume the number of users in one cell is equal to the number of antennas they are equipped with which is not a reasonable assumption. In the next section, we propose a method to choose N users from the K users in the cell. With such a method, the above assumption becomes acceptable.

Table 3.1: Simulation parameters of ZF algorithm

Number of antennas	2/4
Number of users in one cell	2/4
Modulation order	2,4,8,16,32,64
Family of modulation	QAM

Comparing Figure 3.4 and Figure 3.5, we can observe that while the number of transmit antennas increases, the rate of the system increases proportionally. However, the performance of the proposed algorithm gets worse. More users are allowed to transmit data at the same time, such that the level of influence of interference is higher. Although the number of degrees of freedom (number of transmit antennas) also increases proportionally, the performance still degrades slightly.

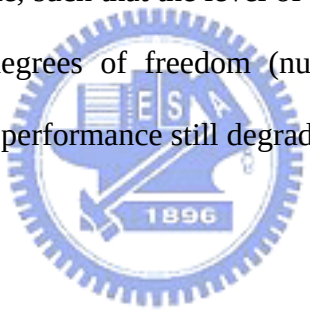

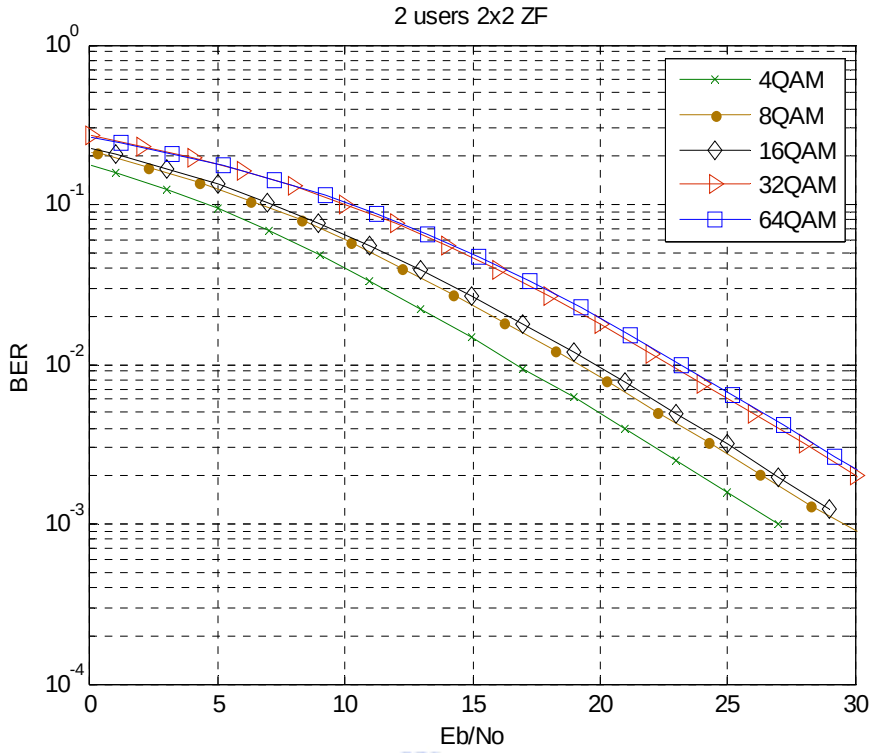

Figure 3.4: BER performances of 2x2 ZF algorithm

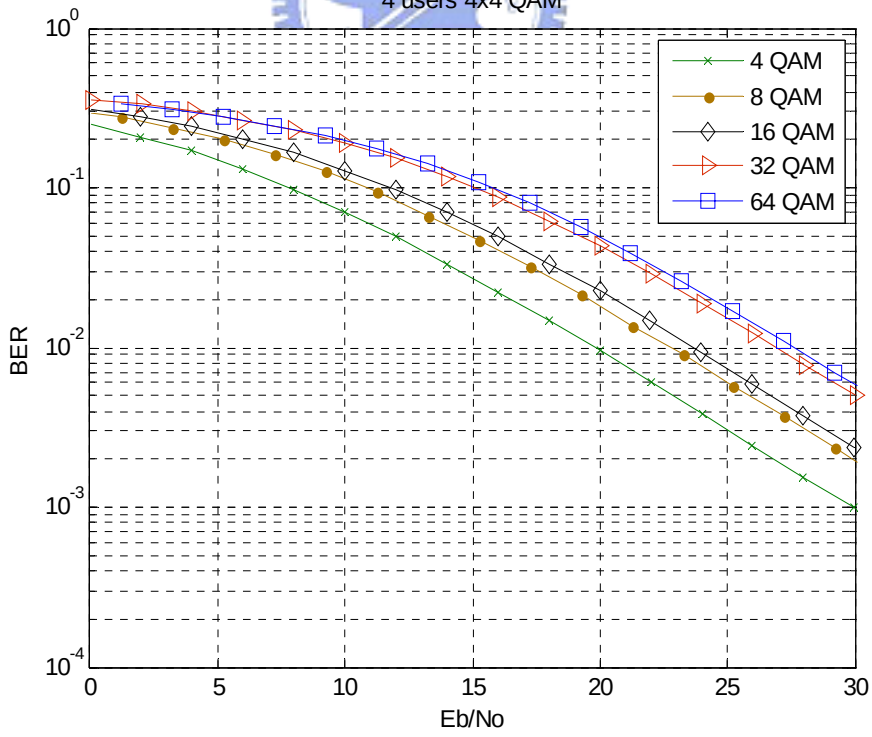

Figure 3.5: BER performances of 4x4 ZF algorithm

3.4 Algorithm of Subcarrier Selection with Beamforming

In the above section we introduce an algorithm of designing beamforming vector to null interference. With this approach applied, we can find a good method to choose subcarriers for each user to transmit data streams. In this section, we propose a method to maximize total transmission rate with each user's BER constraint satisfied. The block diagram is shown in Figure 3.6. We also extend the single carrier problem to multicarrier problem.

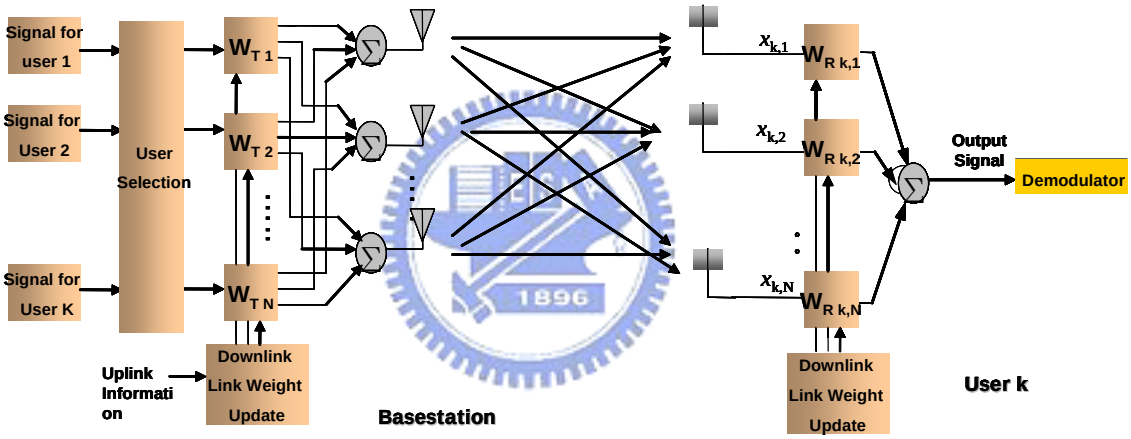

Figure 3.6: Block diagram of beamforming aided subcarrier selection in single carrier case

From the gap approximation [40], the relation between the modulation order and the SNR under BER constraint can be expressed as

$$b = \log_2(1 + \frac{\text{SNR}}{\Gamma}) \tag{3.17}$$

where

$$\Gamma = \frac{1}{1.6}\ln(\frac{0.2}{\text{BER}}). \tag{3.18}$$

The above approximation is applied for M-QAM modulation. We find that this

approximation is tight to within 1 dB at the BER less than 10^{-3}. If the BER constraints are the same for all users, there exists a one-to-one mapping between the SNR and the modulation order. Therefore, the total number of transmit bits in one subcarrier can be written as

$$\begin{aligned} b &= \sum_{i=1}^{N} b_i = \sum_{i=1}^{N} \log_2(1+\frac{\mathrm{SNR}_i}{\Gamma}) \\ &= \log_2(\prod_{i=1}^{N}(1+\frac{\mathrm{SNR}_i}{\Gamma})) \\ &\cong \log_2(\prod_{i=1}^{N}\frac{\mathrm{SNR}_i}{\Gamma}) \end{aligned} \quad . \tag{3.19}$$

Observing the above equation, we find that the rate is proportional to the product of SNRs. For this reason, we choose the product of SNRs as the metric of the system performance. With ZF beamforming, the SNR of user k is $\alpha_k^2/(\left\|\mathbf{w}_{T_k}\right\|^2\sigma_n^2)$ which makes the product of SNRs become $\prod_{i=1}^{N}(\alpha_i^2/\left\|\mathbf{w}_{T_i}\right\|^2\sigma_n^2)$. So $\prod_{i=1}^{N}(\alpha_i^2/\left\|\mathbf{w}_{T_i}\right\|^2)$ is the metric for choosing which users could occupy this subcarrier. The detail procedure is described in the following steps:

ZF Beamformer Aided Subcarrier Selection Algorithm

Step 1) Choose any N users from K total users. Calculate $\prod_{i=1}^{N}(\alpha_i^2/\left\|\mathbf{w}_{T_i}\right\|^2)$ for each selection.

Step 2) Choose the maximal one. Let the selected users transmit data on this subcarrier.

Step 3) Do the above two steps for each subcarrier. Finally, the result of subcarrier allocation indicates which users can occupy each subcarrier. On the other hand, it also shows which subcarriers can be used by one user. In addition, the result makes each subcarrier occupied by N users.

3.5 Computer Simulations

Figure 3.7 shows the simulation results of the beamforming aided subcarrier selection algorithm. Here each user is equipped with two antennas such that each subcarrier only can be occupied by two users. The number of candidates is larger such that more multiuser diversity can be obtained. Channel model is assumed as independent Rayleigh fading channel. As shown in Figure 3.7, we find that when the number of candidates is larger, the BER curve behaves more like that under the AWGN channel. Because we always choose the two best users to occupy the subcarrier, the shape of distribution of selected path gain becomes narrow. As the number of candidates approaches infinity, the shape of distribution of selected channel fading gain becomes like an impulse. Hence its BER curve approaches that under the AWGN channel.

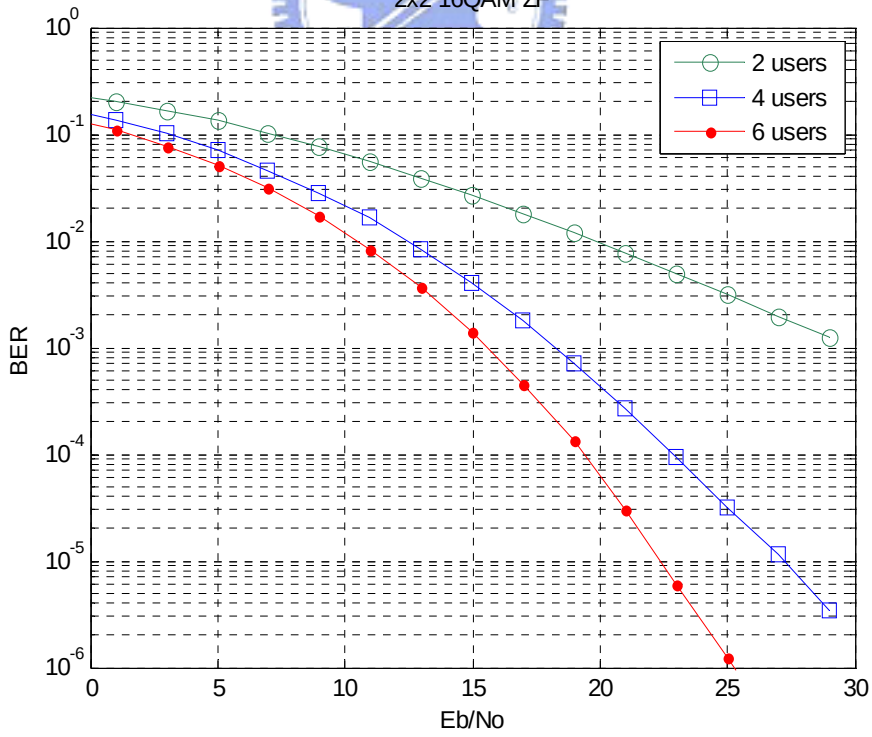

Figure 3.7: BER performances of beamforming aided subcarrier selection with 2x2 antennas and 16QAM modulation

3.6 Summary

In this chapter, we propose a ZF beamforming design algorithm to null the interference between users in multiuser MIMO systems. SVD decomposition is utilized to simplify our design procedure. Finally, with the ZF beamforming design method, a subcarrier selection algorithm is proposed in order to maximize the total transmission rate under the BER constraint. The simulation result shows that the performance improves significantly due to multiuser diversity.

Chapter 4

Multiuser Adaptive Power and Bit Allocation for OFDM Systems

In multicarrier systems, a loading algorithm is used to allocate bits and power to subchannels. This task is a constrained optimization problem and two cases are of interest, namely, margin maximization and rate maximization.

Margin maximization is equivalent to power minimization subject to a fixed target rate; and rate maximization is equivalent to rate maximization subject to a fixed target power. In both cases, system specifications impose additional constraints including total power budget, power spectral density mask, maximum bit error rate, integer bit assignments, and maximum size of the embedded QAM constellations. Although there are several single-user bit-loading algorithms, not all of them are optimal under the integer bit constraint, and not all of the above constrains are encountered in the problems.

In [41]-[43], the bit-loading solution is generally noninteger; therefore, a suboptimal integer rounded bit allocation is provided. In [44]-[45], the discrete bit-loading problem is addressed using an iterative bi-filling or bit-removal procedure based on a subchannel-cost criterion for a total power budget constraint. We will review these methods in Section 4.2.1.

In this chapter, we propose a computationally efficient discrete bit-loading algorithm for single-user margin maximization problem. The new algorithm exploits the differences between the subchannel gain-to-noise ratios measured during channel training in order to calculate an initial bit allocation and then performs a bit-removal algorithm with fewer candidates to reach the optimal target-rate solution.

This chapter is organized as follows. Section 4.1 formulates the bit and power loading problem in mathematical form and describes the system model. In Section 4.2, we review the conventional method for solving bit and power loading problem. After that, we present the new bit loading algorithm in detail. Finally Section 4.3 gives the simulation result of the proposed algorithm.

4.1 System Model and Problem Formulation

The choice of constellations (and equivalently, of the allocated power) is considered for transmission over a set of parallel subchannels:

$$y_i = \sqrt{P_i}\alpha_i x_i + n_i, \qquad 1 \le i \le N \tag{4.1}$$

where $\mathrm{E}[x_i x_j^*] = \delta_{ij}$ and $\mathrm{E}[n_i n_j^*] = \sigma^2 \delta_{ij}$. The CNR (channel gain to noise ratio) of the ith subchannel is given by $\mathrm{CNR}_i = |\alpha_i|^2 / \sigma^2$.

We want to minimize the total transmit power subject to satisfy user's rate and BER requirements. The problem can be formulated as

$$\begin{aligned} &\text{minimize} \quad \sum_{i=1}^{N} P_i \\ &\text{subject to} \quad \sum_{i=1}^{N} b_i = B_{\text{req}}, b_i \in \{0,1,...,\bar{b}\}, \forall 1 \le i \le N \\ &\qquad\qquad \mathrm{BER}_i = \mathrm{BER}_{\text{req}} \end{aligned} \tag{4.2}$$

where $\bar{b}$ is the maximum number of bits that can be assigned in the system. In order to simplify the problem, we use the BER approximation as

$$\mathrm{BER} = 0.2 \times \exp\left(\frac{-1.6 \times P \times \mathrm{CNR}}{2^b - 1}\right) \tag{4.3}$$

where *b* means modulation order. This approximation is applied for M-QAM and the error is less than 1 dB at the BER less than 10^{-3}.

4.2 Power and Bit Allocation Algorithm

In this section the waterfilling solution from the view point of the capacity is first introduced. The modified form, gap approximation, is also recommended. After that, we review the conventional power and bit allocation algorithms and point out the drawbacks and advantages of the conventional algorithms. Finally, the proposed algorithm is described which combines the advantage of the conventional methods.

4.2.1 Conventional Power and Bit Allocation Algorithm

In this part, two kinds of famous conventional power and bit allocation algorithms are introduced. The first one is a capacity-like approach whose solution is continuous. So the final bit distribution is rounded from the continuous waterfilling solution. The second one is a greedy algorithm. It tries to find the power change after adding or removing one bit on subcarriers. Find the minimal cost bit and to add or remove iteratively it until rate requirement is achieved.

4.2.1.1 Gap-Approximation with Water-Filling Solution

We start this part with well-known capacity achieving solution since the following methods are strongly based on it. From the landmark work by Shannon in 1948, the achievable information rate through a channel with a given SNR is given by

$\log_2(1+\text{SNR})$ bits/transmission. For the set of parallel subchannels in Equation (4.1), the achievable information rate is given by the sum $\sum_{i=1}^{L}\log_2(1+p_i\lambda_i)$, and the capacity is given by the maximum achievable rate over all possible power allocation strategies $\{p_i\}$. The optimum power distribution is the well-known waterfilling solution:

$$P_i = \max(0, \mu - \frac{1}{\alpha_i^2}) \quad 1 \le i \le N, \tag{4.4}$$

where μ is the waterlevel chosen to satisfy the power constraint (the waterlevel can be alternatively chosen to satisfy rate requirement with minimum power)

To achieve the channel capacity, however, it is necessary to use ideal Gaussian codes, which are not practical for real systems, hence the need to employ simpler and more practical constellations such as QAM or pulse amplitude modulation (PAM).

So we use the gap approximation. The basic idea of the gap approximation is to avoid the need for ideal Gaussian codes inherent in the capacity-achieving solution. Instead, a family of practical constellations, such as QAM or PAM, is employed. The number of bits that can be transmitted for a given family of constellations and a given probability of detection error P_e is approximately given by $\log_2(1+\text{SNR}/\Gamma)$, where $\Gamma \ge 1$ is the gap which depends only on the family of constellations and on P_e. Interestingly, there is a constant gap between the Shannon capacity and the spectral efficiency of realistic constellations, which can be interpreted as a penalty for not using ideal Gaussian codes. For QAM constellations, for example, the number of bits at each subchannel is given by

$$b_i = \log_2(1+\frac{P_i \cdot CNR_i}{\Gamma}). \tag{4.5}$$

This expression is like the capacity expression. So the first conventional power and bit allocation algorithm solution is the waterfilling solution. The solution can be written as

$$P_i = \max(0, \mu - \frac{\Gamma}{\alpha_i^2}) \quad 1 \le i \le N . \tag{4.6}$$

This solution is continuous; hence, rounded distribution is the solution of the first conventional algorithm. This procedure is simple however the solution is not optimal.

The second conventional method is the greedy algorithm. From gap approximation we can find power increment with one bit increment per subchannel and power decrement with one bit remove per subchannel. The bit-filling algorithm starts from an initial all-zeros bit allocation ($b_i = 0$ for $1 \le i \le N$) and adds one bit at a time to the subchannel that requires the minimum additional power until the target rate is achieved. On the other hand, the bit-removal algorithm starts from an initial maximum bit allocation and removes one bit at a time from the subchannel that saves the maximum power until the target rate is achieved.

The logarithmic rate expression in Equation (4.5) is a strictly increasing and concave function of P_i and vanishes at P_i=0. These conditions guarantee the optimality of the above greedy bit-filling and bit-removal methods. Moreover, it can be proved that both methods result to the same bit allocation. However, the computational load associated with each algorithm depends mainly on the requested target rate. If B_{req} is closer to the rate achieved by the $\bar{b}$ allocation, then bit-removal converges faster. These methods are optimal but complex.

4.2.2 Proposed Power and Bit Allocation Algorithm with Low Complexity

In this section we will propose a new power and bit allocation algorithm which combines the advantages of the above two conventional algorithms which are optimal and computationally efficient.

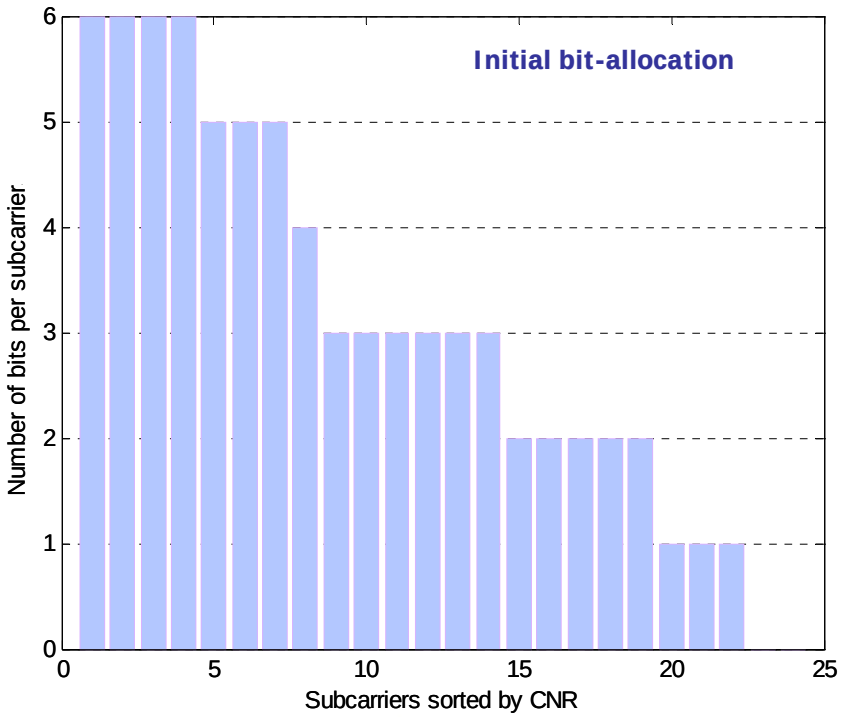

Figure 4.1: Bit distribution after initial allocation

Our bit loading algorithm uses a two-step procedure to obtain the optimal bit allocation. Initially, the algorithm exploits the differences between the CNRs of subcarriers and calculates the initial bit allocation under the system constraints, as shown by the initial bit-allocation curve in Figure 4.1. The result shows that it has no more than a single bit difference per subchannel compared with the optimal bit distribution as shown in Figure 4.2. Then, bit-removal is used in order to achieve the target-rate bit allocation as shown in Figure 4.3.

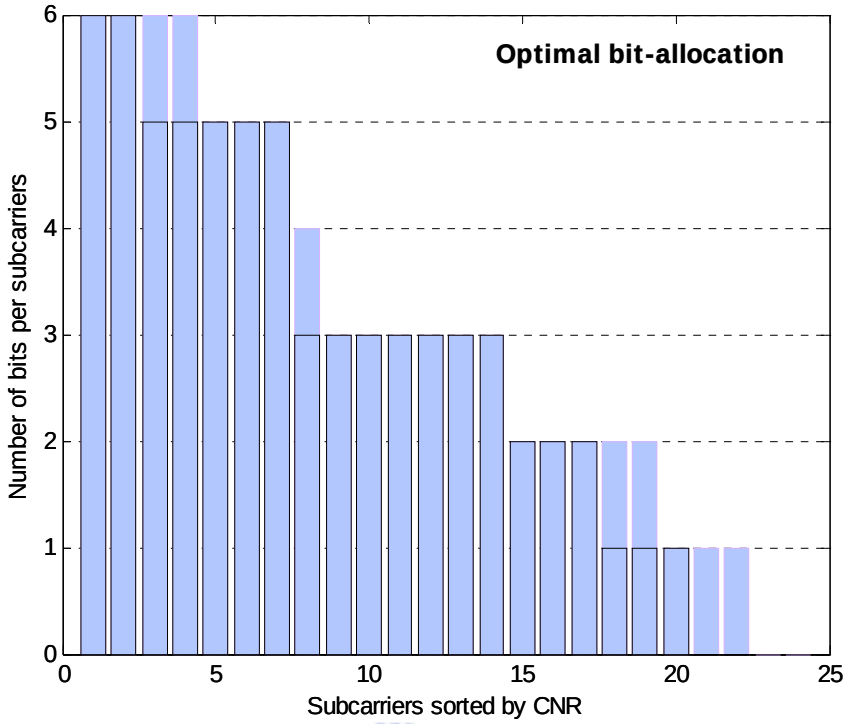

Figure 4.2: Comparison between optimal and the initial allocation

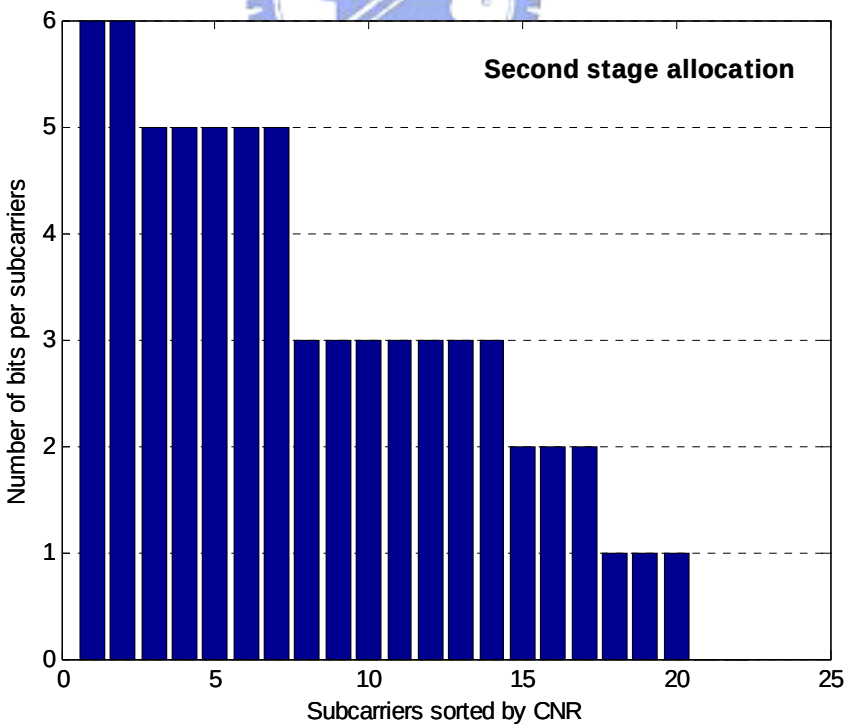

Figure 4.3: Bit distribution after second stage allocation

From Equation (4.5), the power increment to transmit one more bit on subcarrier i carrying b_i bits is given by

$$\Delta P_i^+(b_i) = \frac{\Gamma}{\mathrm{CNR}_i} 2^{b_i} . \tag{4.7}$$

The power decrement by removing one bit is given by

$$\Delta P_i^-(b_i) = \frac{\Gamma}{\mathrm{CNR}_i} 2^{b_i - 1}, \tag{4.8}$$

where $\Gamma = \frac{1}{1.6}\ln(\frac{0.2}{\mathrm{BER}})$ is constant under the BER constraint.

The case of two subcarriers is considered first. We examine the process of bit-filling. Without loss of generality, $\mathrm{CNR}_m > \mathrm{CNR}_n$ is assumed. We find that bit-filling loads subchannel m with $b_m = \lfloor \log_2(k_m) + 1 \rfloor$ bits before the first bit is added to subchannel n as shown in Figure 4.5(I), where $k_m = (\mathrm{CNR}_m)/(\mathrm{CNR}_n)$ and b_m is the integer solution to

$$\Delta P_m^+(b_m - 1) \le \Delta P_n^+(0) \le \Delta P_m^+(b_m) \tag{4.9}$$

Then, any additional bits with respect to subchannels m and n are successively added, starting from subchannel m as seen in Figure 4.5 (II)-(V). The above statement is valid, since for any integer $x \ge 0$

$$\Delta P_m^+(b_m - 1 + x) \le \Delta P_n^+(x) \le \Delta P_m^+(b_m + x) . \tag{4.10}$$

We can calculate the difference of number of bits between these two subcarriers, which is

$$d_n = b_m - 1 = \left\lfloor \log_2(\frac{\mathrm{CNR}_m}{\mathrm{CNR}_n}) \right\rfloor . \tag{4.11}$$

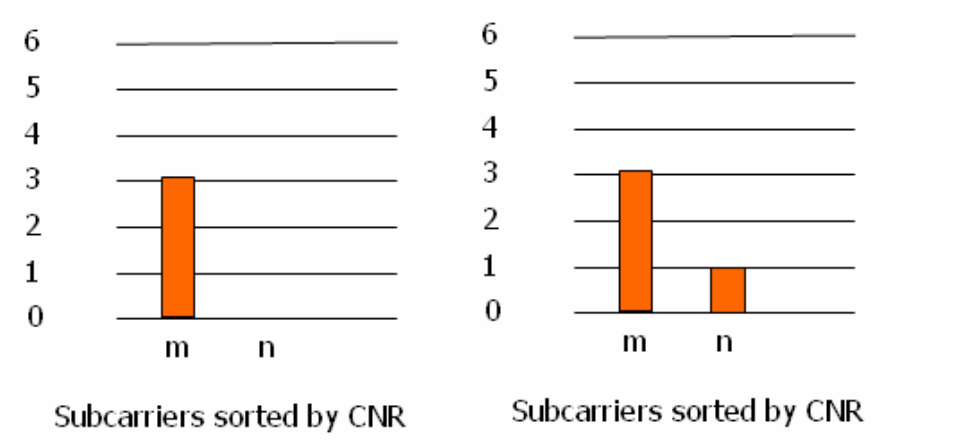

(I) (II)

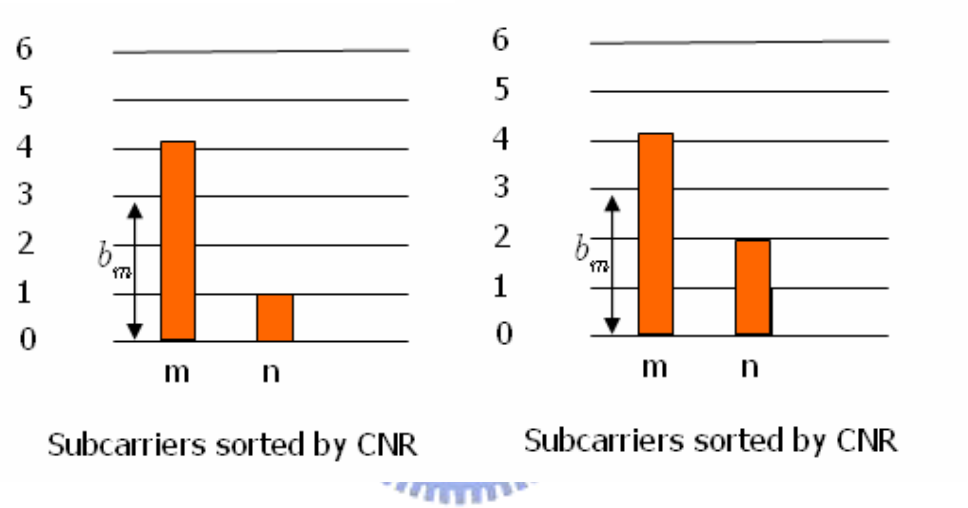

(III) (IV)

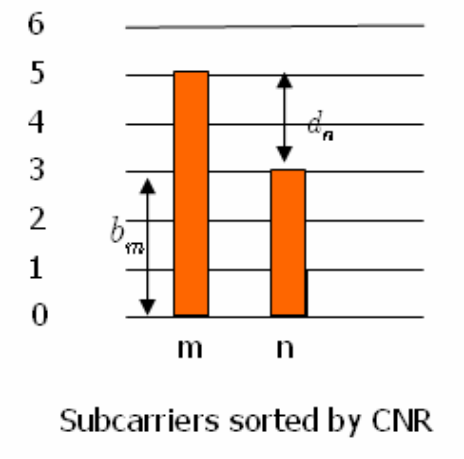

(V)

Figure 4.4: Procedure of bit-filling algorithm in two subcarrier case

Similarly, we examine bit allocation on subchannels *p*, *m* and *n* ,where $CNR_p \geq CNR_m \geq CNR_n$. Bit-filling algorithm adds $b_n = \lfloor \log_2(k_n) + 1 \rfloor \geq b_m$ bits to subchannel *p* before the first bit is added to subchannel *n*, where $k_n = (CNR_p / CNR_n)$, while subchannel *m* is filled with $b_n - b_m$ bits. The last statement is straightforward by setting $x = b_n - b_m$ in Equation (4.10). Then, any additional bits with respect to subchannels *p*, *m*, and *n* are inserted based on the minimum required power, so that, after every three allocations on subchannels *p*, *m*, and *n*, they are filled with one more bit. In the following examples, the above results are extended to all *N* subchannels. This algorithm can be illustrated by Figures 4.5 and 4.6 which describe the first and second stage algorithm in detail.

A. Initial bit allocation

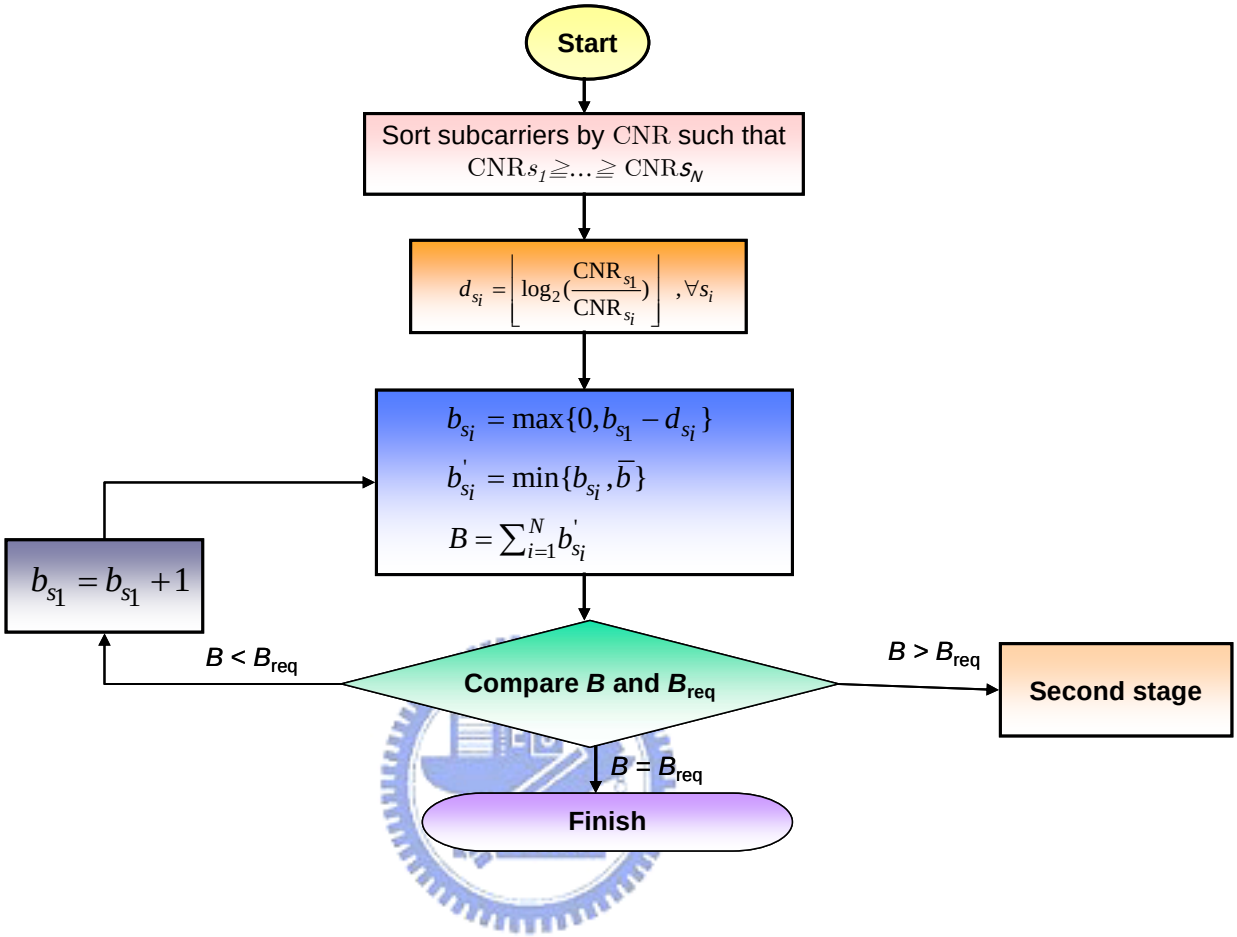

Figure 4.5: Flow chart of initial stage of proposed bit loading algorithm

B. Second Stage

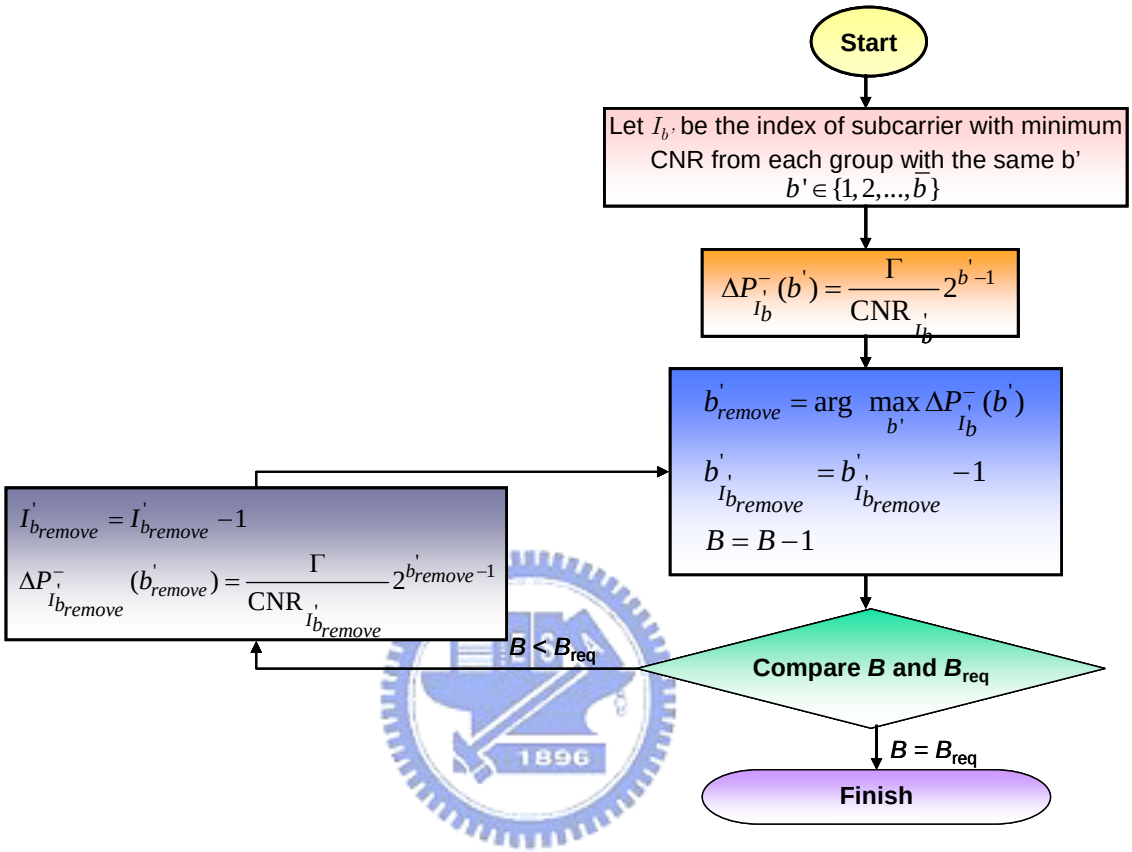

Figure 4.6: Flow chart of second stage of proposed bit loading algorithm

An example is given to make the algorithm easy to understand. Consider that the rate requirement is 58 bits per OFDM symbol which is denoted as B_{req}. The total number of subcarriers is 30 and CNR_i denotes channel gain-to-noise ratio on subcarrier *i*. In the following figures, x-axis represents the index of sorted CNR and y-axis represents the number of allocated bits. The result of each step is shown in Figure 4.7 where *B* stands for the number of total assigned bits.

Initial Stage:

The initial value of b_{s_1} is 4. The bar masked by gray region represents the number of bits allocated to subcarriers. In Figure 4.7(I), we can find that the number of total assigned bits in the first allocation is 16. In order to make the number of total assigned bits larger than required, we down shift the gray block by one bit in each iteration. We then recalculate the number of assigned bits iteration by iteration until the number of total assigned bit is more than required as shown in Figure 4.7(II)-(V).

Second Stage:

In the second stage, bit-removal processing is executed. We select the subcarriers with the minimum CNR from each group which has the same number of allocated bits. It is shown by arrows in Figure 4.7 (VI)-(VII). We find that these subcarriers are the right most ones in each group which have the same number of assigned bits. We calculate their power decrement by removing one bit on these subcarriers. Choosing the maximal one, remove one bit from it and shift the red arrow left. We then subtract the total assigned bit by one and iterate the loop until the number of total assigned bits is equal to required. Finally optimal bit allocation is obtained with the power minimization goal met.

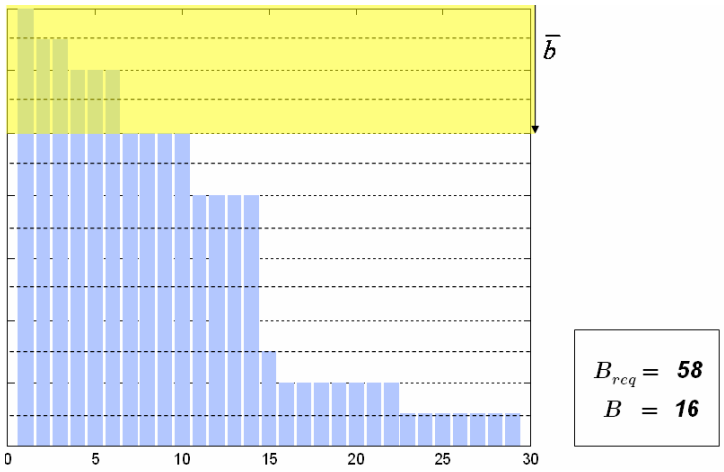
$\bar{b}$
0
5
10
15
20
25
30
$B_{req} = 58$
$B = 16$

(I)

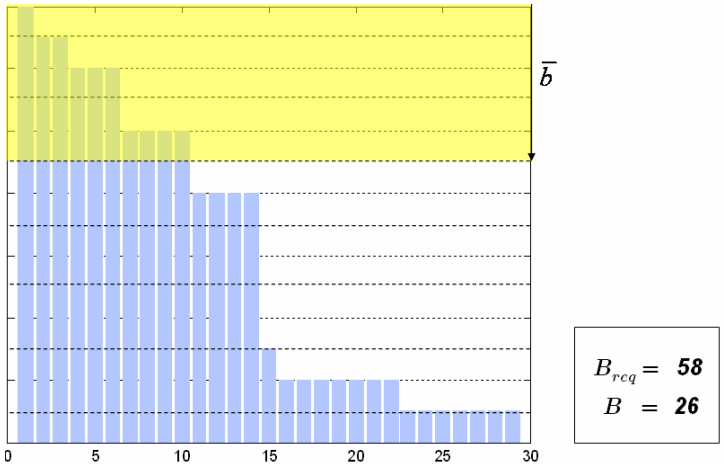
$\bar{b}$
0
5
10
15
20
25
30
$B_{req} = 58$
$B = 26$

(II)

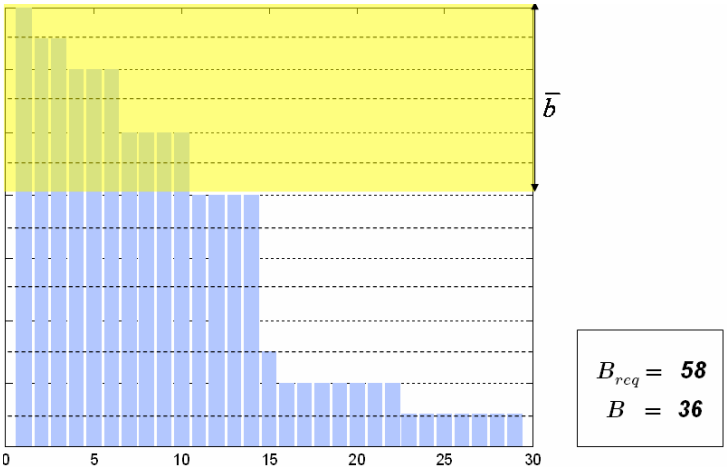
$\bar{b}$
0
5
10
15
20
25
30
$B_{req} = 58$
$B = 36$

(III)

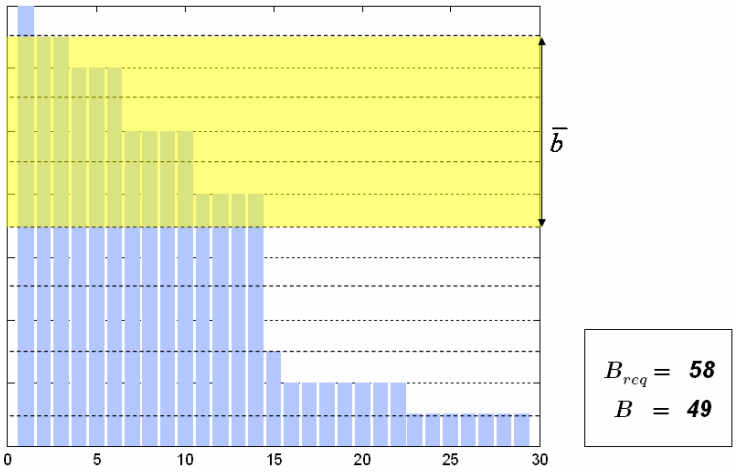
$\bar{b}$
0
5
10
15
20
25
30
$B_{req} = 58$
$B = 49$

(IV)

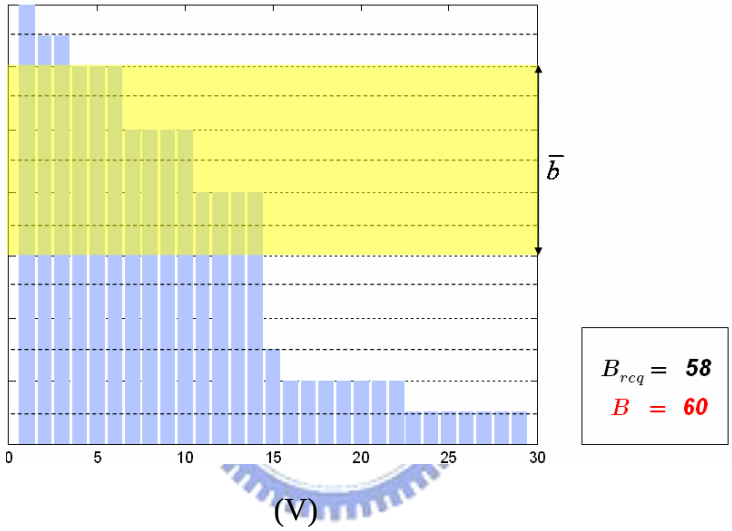
$\bar{b}$
0
5
10
15
20
25
30
$B_{req} = 58$
$B = 60$

(V)

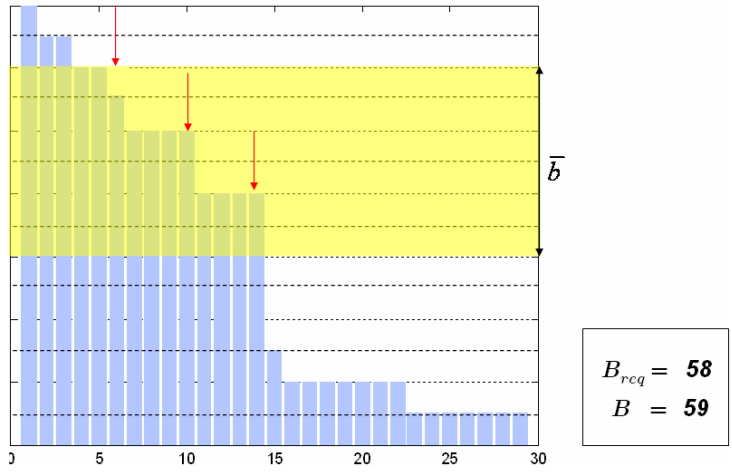
$\bar{b}$
0
5
10
15
20
25
30
$B_{req} = 58$
$B = 59$

(VI)

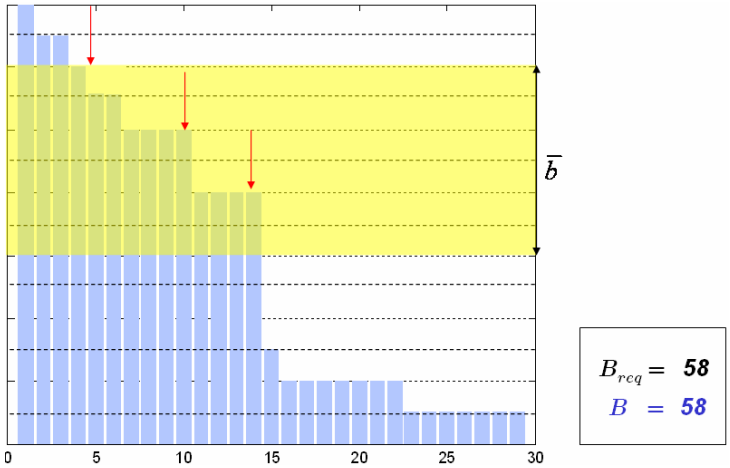

(VII)

Figure 4.7: Example of proposed bit loading algorithm

4.3 Complexity Analysis

In this section, we analyze the complexity of the proposed bit and power loading algorithm. This results are compared with the bit-filling and bit-removal algorithm adopted in [50], [53], and [54]. For these two methods, they require one logarithmic operation and three multiplications for initialization and one exponential operation and two multiplications for each iteration. The proposed algorithm requires one logarithmic operation, one exponential operation and two multiplications for initialization of each subcarrier; subsequently it no longer requires any complex operations in each iteration. The detail description is shown in Table 4.1.

An example is given to make the complexity easy to compare. Consider that the rate requirement is 512 bits per OFDM symbol and the total number of subcarriers is 128; maximal number of bits can be assigned is 6. The results are shown in Table 4.2 where we observe the total number of logarithmic and exponential operations of the proposed algorithm is fewer than that of other algorithms. Besides, the proposed algorithm requires considerably fewer number of multiplications.

Table 4.1: Complexity of proposed bit and power loading algorithm compared with other conventional algorithms

	Logarithm	Exponent	Multiplier
Bit-filling	1	B_{req}	$2B_{\text{req}}+3$
Bit-removal	1	$N\bar{b}-B_{\text{req}}$	$2(N\bar{b}-B_{\text{req}})+3$
Proposed	N	N	$2N+3$

Table 4.2: Example of complexity analysis

	logarithm	exponent	multiplier
Bit filling	1	512	1027
Bit removal	1	256	515
Proposed	128	128	259

4.4 Computer Simulations

The simulation results are shown in the following figures. Figure 4.8 compares the BER performance of adaptive modulation with fixed modulation where the bits requirement per OFDM symbol is 128 bits and the number of subcarriers is 32. Hence the fixed modulation order is 4 in order to compare on a fair basis. It is observed that the performance of adaptive modulation has enormous improvement compared with that of nonadaptive modulation.

Figure 4.9 shows the BER curve with different bit requirements. Because the gap approximation is tighter while for $\text{BER} \le 10^{-2}$, we only show the performance in this range. From the figure, we find that the effect of different bit requirement on BER

curve is just a horizontal shift. The gap between two adjacent curves is about 2 dB.

Figure 4.10 gives the BER curves with different BER constraints with the understanding that gap approximation is an approximated equation describing the relation between BER and power. The results show that the average BER is always lower than the original BER constraint.

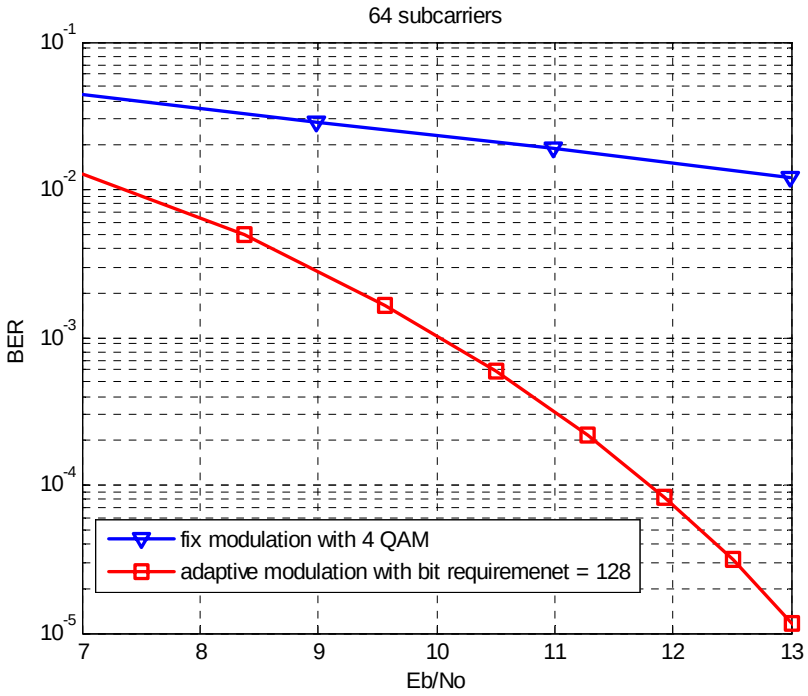

Figure 4.8: BER performance of adaptive bit and power allocation compared with fixed modulation

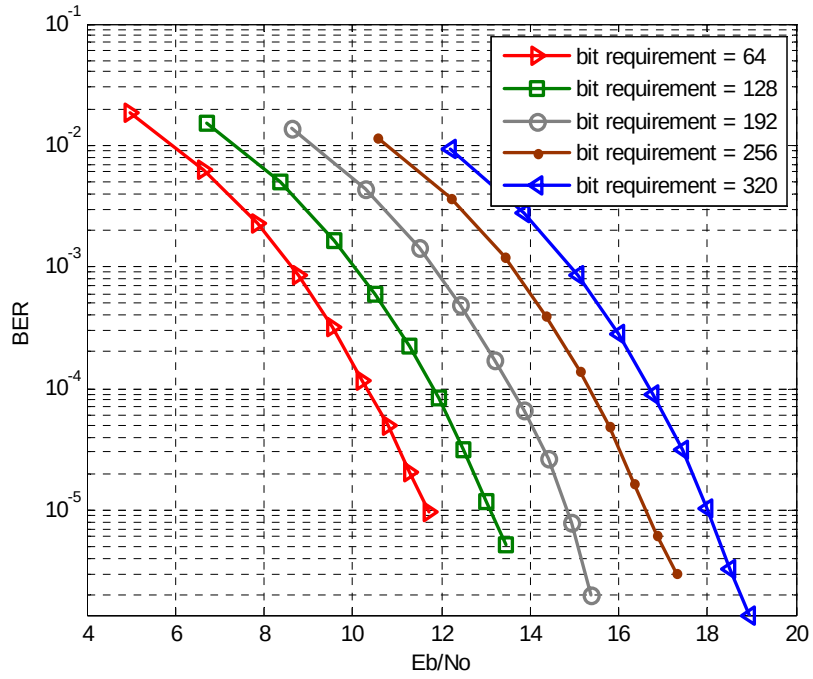

Figure 4.9: BER performances of proposed bit loading algorithm with different bits requirements

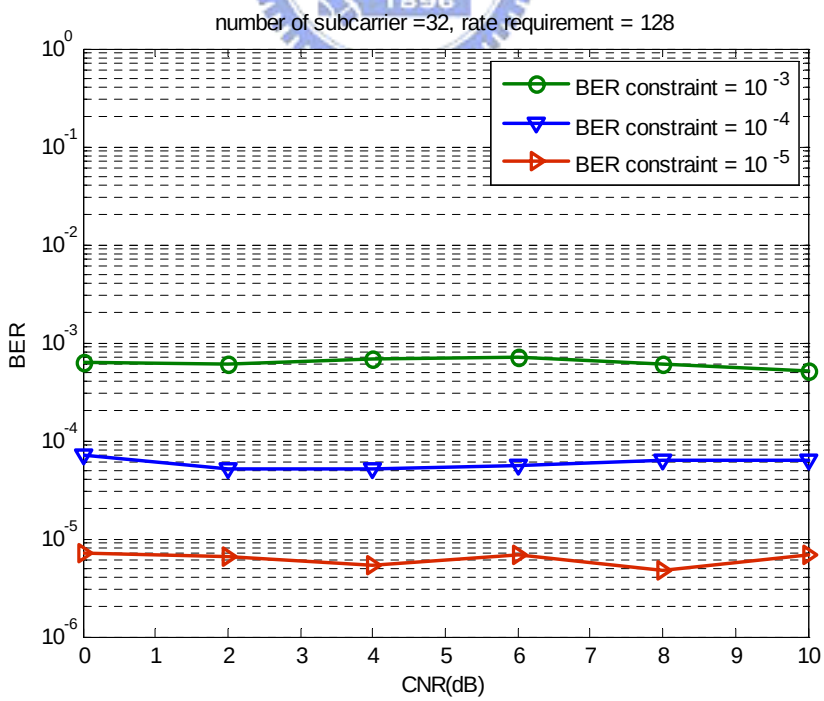

Figure 4.10: BER performances of proposed bit loading algorithm with different BER constraints

4.5 Summary

The new bit-loading algorithm proposed in this chapter provides the optimal discrete solution to the power minimization problem under QoS constraints including BER and rate requirements. It also takes into account that $\bar{b}$ upper bounds the system. In addition, it requires less computational complexity compared to the optimal bit-filling and bit-removal algorithms. The proposed algorithm exploits the subchannel gain-to-noise ratio levels in order to calculate a loop representative bit-allocation profile and then uses a multiple-bits insertion that results in faster convergence to the target rate. Finally, simulation results confirm the efficiency of the proposed algorithm.

Chapter 5

Beamforming Aided Multiuser Adaptive Radio Resource Management

In Chapter 5, an adaptive radio resource-management algorithm for multiuser transmission in MIMO-OFDM systems is proposed. The objective of this algorithm is to: 1) exploit the inherent system diversities including time, frequency, space, and multiuser diversities; 2) minimize the overall transmit power; 3) instantaneously guarantee the fulfillment of each user's QoS requirements including BER and rate requirements. To be more specific, the proposed algorithm optimizes transmit and receive beamforming, subcarrier allocation, power and bit distribution for all users jointly according to the instantaneous CSI and QoS requirements.

This chapter is organized as follows. Section 5.1 formulates the problem of beamforming aid multiuser adaptive radio resource management and proposes an algorithm to solve it, subsequently signaling model in practical wireless communication system is described in Section 5.2. Finally simulation results of the proposed algorithm are shown in Section 5.3.

5.1 Proposed Beamforming Aided Multiuser Radio Resource Management Algorithm

The problem we consider about in multiuser MIMO-OFDM systems where each user and base station are equipped with the same number of antennas; it try to decide how many users can occupy the same subcarrier at the same time. Our objective is to minimize the total transmit power while satisfying each user's QoS constraints including rate and BER requirements. This problem can be formulated as follows:

$$\begin{aligned} &\text{minimize} \quad \sum_{i=1}^{K}\sum_{j=1}^{N} P_{i,j}\delta_{i,j} \\ &\text{subject to} \quad \sum_{j=1}^{N} b_{i,j}\delta_{i,j} = B_{i,\text{req}}; \\ &\qquad \text{BER}_{i,j} = \text{BER}_{\text{req}}, \quad \forall 1 \le i \le K \\ &\qquad b_{i,j} \in \{0,1,\ldots,\bar{b}\}; \\ &\qquad P_{i,j} \ge 0, \quad \forall\, 1 \le i \le K,\ 1 \le j \le N \end{aligned} \tag{5.1}$$

where $\bar{b}$ is the maximal number of bits that can be assigned in the system and $\delta_{i,j}$ is the subcarrier indicator whose value is defined as

$$\delta_{i,j} = \begin{cases} 1, & \text{if subcarrier } j \text{ is assigned to user } i \\ 0, & \text{otherwise} \end{cases} . \tag{5.2}$$

In order to achieve our objective, the proposed algorithm optimizes transmit and receive beamforming, subcarrier allocation, power distribution, and bit distribution for all users jointly according to the instantaneous CSI and QoS requirements.

Based on the beamforming aided subcarrier allocation algorithm proposed in Chapter 3, we assign each user subcarriers to transmit data and decide the transmit and receive beamformers on each subcarrier in order to null the interference between users. After the procedure of beamforming and subcarrier assignment, the bit and power loading algorithm proposed in Chapter 4 is applied to allocate the bit and power for

each user in order to minimize the total transmit power with each user's QoS constraints met. The detail procedure of the algorithm is described in the following steps:

Beamforming Aided Multiuser Adaptive Radio Resource Management Algorithm

Step 1) Choose any *N* users from *K* total users. For each selection, $\mathbf{H} = \sum_{k=1}^{N} \mathbf{u}_k \alpha_k \mathbf{v}_k^H$ is the channel matrix composed of allowed users' channel matrices, transmit weight vector is calculated by $\mathbf{w}_{T_k} = \mathbf{v}_k$ and receive weight vector is calculated by $\mathbf{w}_{R_k} = \left[\mathbf{e}_k^T \cdot \mathbf{u}_k^{-1}\right]^H$; then calculate $\prod_{k=1}^{N} (\alpha_k^2 / \left\|\mathbf{w}_{T_k}\right\|^2)$ as the metric for choosing which users could occupy this subcarrier.

Step 2) Choose the maximal one and let selected users transmit data on this subcarrier.

Step 3) Do the above two steps for each subcarrier. Finally, the result of subcarrier allocation indicates which users can occupy each subcarrier. On the other hand, it also shows which subcarriers can be used by one user.

Step 4) For each user, implement the bit and power loading algorithm proposed in Chapter 4 with the assigned subcarriers and QoS.

The transceiver block diagram of beamforming aided multiuser radio resource management algorithm is shown in Figure 5.1; the detail description of the transmitter architecture is illustrated in Figure 5.2.

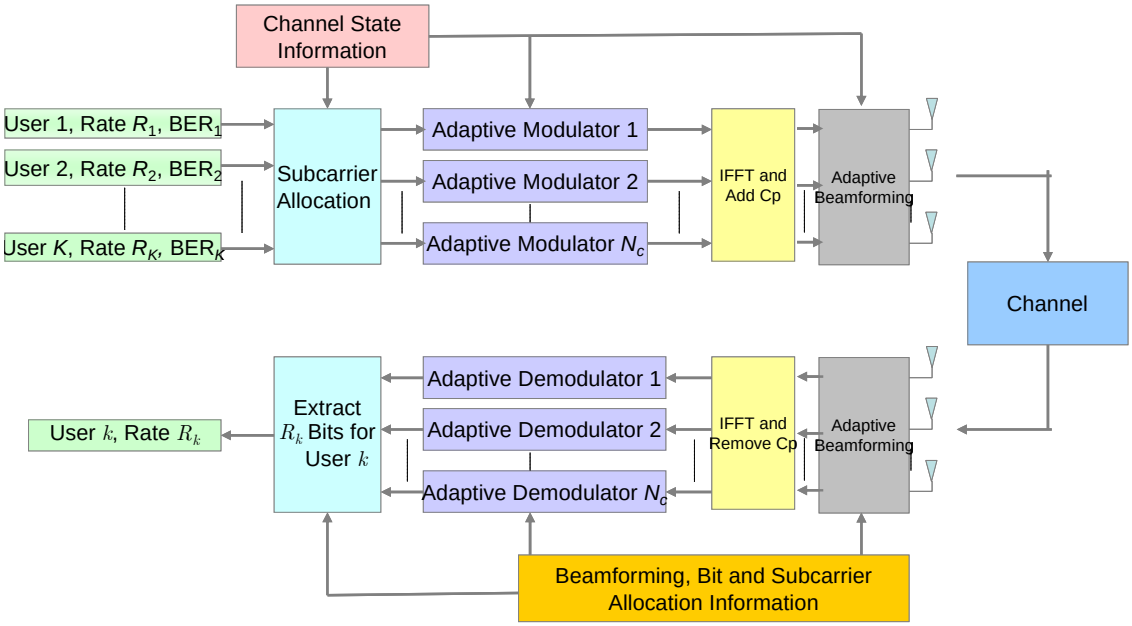

Figure 5.1: Block diagram of downlink multiuser adaptive MIMO-OFDM systems

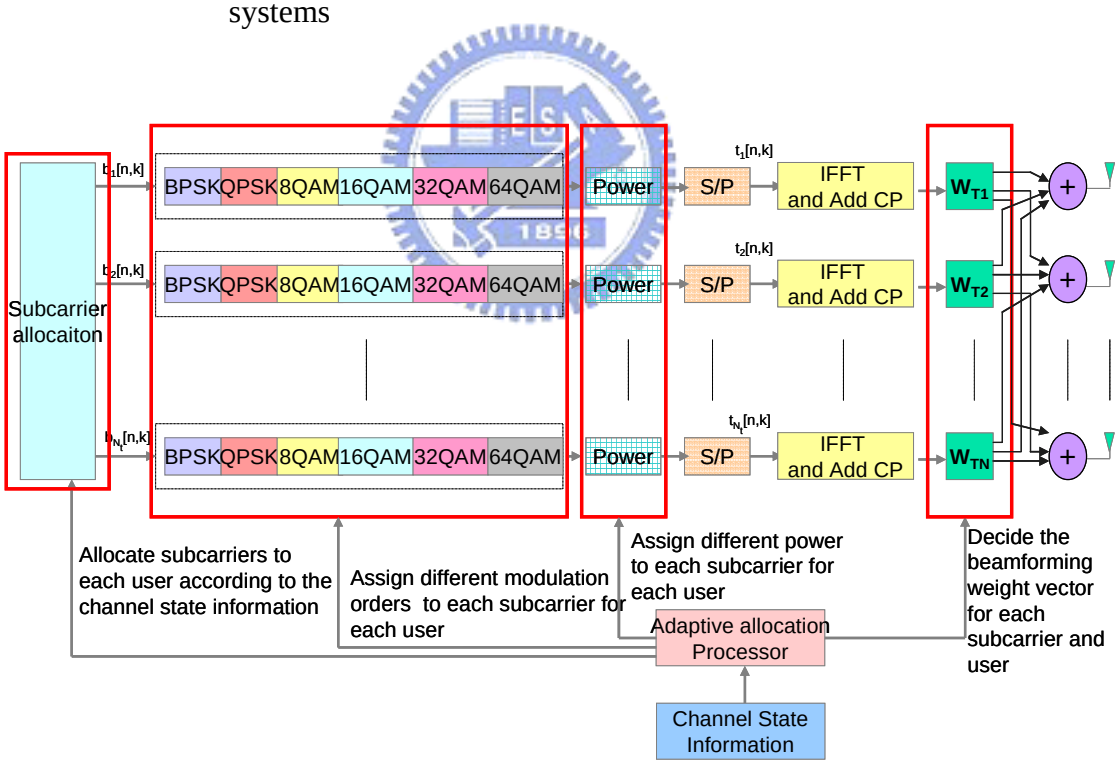

Figure 5.2: Transmitter architecture of beamforming aided radio resource management algorithm

5.2 Signaling Model in Adaptive Scenario

Because the parameters of the proposed algorithm are based on the instantaneous channel state information of all users, obtaining the instantaneous channel state information becomes the most important issue. In this section, we discuss the signaling model in the adaptive scenario. Figure 5.3 illustrates the signaling model for which the system is based upon a time-division duplex (TDD) operation, assuming that the durations of the uplink and downlink timeslots are the same, and are denoted by t_o. Consider the downlink transmission at time t, for example. Assuming that the channel is reciprocal, the BS first predicts the downlink channel of time t based on the uplink frame received at time t-t_0 and then the BS adapts the bit and power allocation accordingly; subsequently the resultant parameters are sent to the mobiles via the control channels. Likewise, the mobile predicts the downlink channel of time t based on the downlink frame received at time t-$2t_0$ and then the mobile adapts the receive beamforming vector. The quality of channel prediction suffers from the changes of the CSI between successive timeslots due to the presence of Doppler spread. Fortunately, in most cases, the channel varies relatively slowly compared with the frame rate. Therefore, the channel can be considered as a quasi-static one, and the channel variation within successive timeslots can be neglected [46].

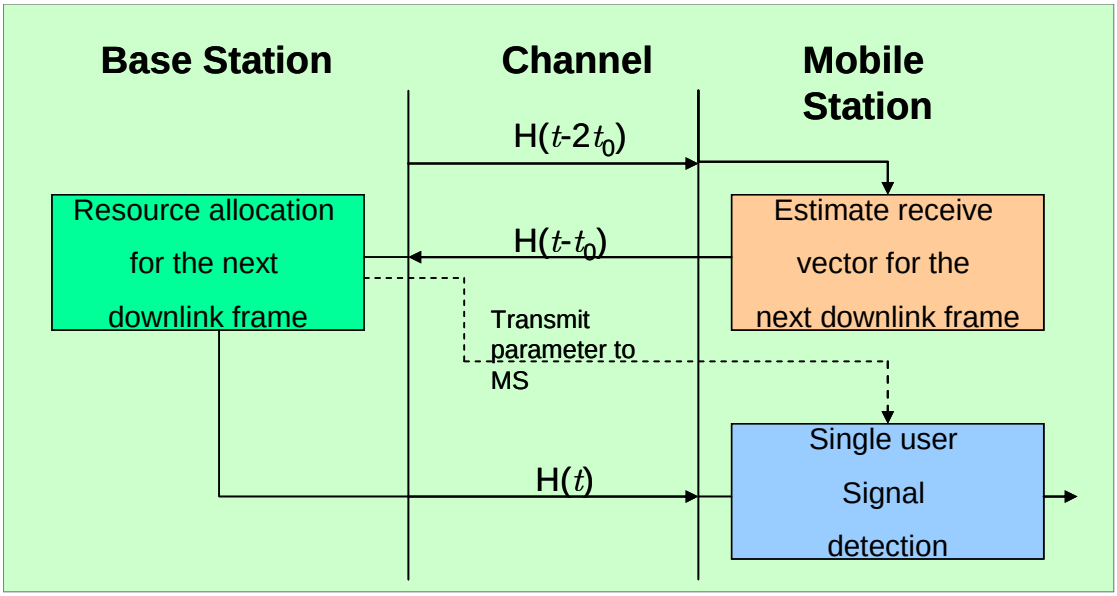

Figure 5.3: Signaling model in adaptive scenario

5.3 Computer Simulations

In this section, computer simulation results are conducted to evaluate the performance of the beamforming aided radio resource management algorithm. Throughout the simulation, we only deal with discrete time signal processing in the baseband; hence pulse-shaping and matched-filtering are not considered for the sake of simulation simplicity. Also, channel estimation and timing synchronization are assumed to be perfect. Table 5.1 lists all parameters used in our simulation. There are 64 subcarriers in the OFDM system and each link in MIMO is modeled as an i.i.d Rayleigh fading channel. The set of QAM constellation used in the simulation is {0, 2, 4, 8, 16, 32, and 64}. There are four users in one cell, and each user and base station are equipped with two antennas.

The BER performances of the beamforming aided multiuser adaptive radio resource management with different rate requirements are shown in Figure 5.4. We observe that the gaps between the different rate requirements with the proposed

algorithm in this chapter are almost the same, equal to about 1.2 dB, whereas the gaps between the different rate requirements in the single user case is about 1.7 dB. Moreover, as the rate requirement increases, the gap between the four user case and single user case becomes larger.

Now, we consider the operations under the situation that only partial CSI is available at the transmitter, but full CSI is available at the receiver. The transmitter acquires channel knowledge either via a feedback channel, or, by channel estimation in a time division duplex (TDD) operation. The partial CSI includes the perfect CSI $\mathbf{H}$ plus a perturbation term $\mathbf{\Delta H}$ with known probability density function (pdf). Figure 5.5 shows BER performances with channel estimation error, where $\tilde{\mathbf{H}} = \mathbf{H} + \mathbf{\Delta H}$ represents the estimated channel at the transmitter. It is assumed that each element in $\mathbf{\Delta H}$ is an i.i.d Gaussian distribution with zero mean and variance σ_e^2 [52]. As seen in the figure, we observe that the performance degradation is acceptable when the variance of channel estimation error is less than 0.01.

Table 5.1: Simulation parameters of beamforming aided multiuser adaptive radio resource management algorithm

Number of subcarriers	64
Maximum number of bits can be assigned	6
Channel model	Rayleigh fading
Number of users	4
Number of transmit antennas	2
Number of receive antennas	2

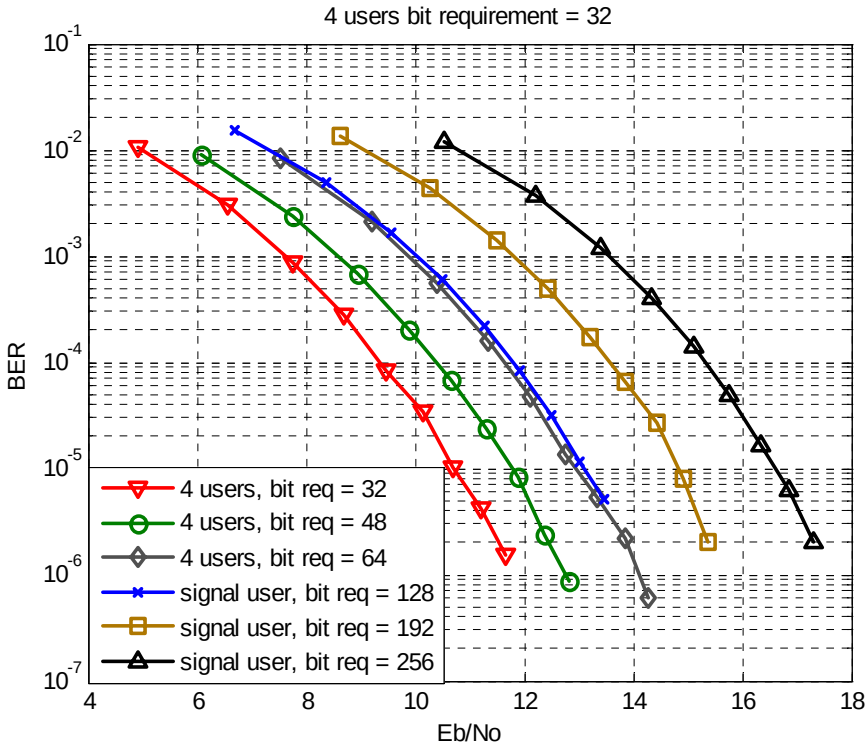

Figure 5.4: BER performances of beamforming aided multiuser resource allocation compared to single user case

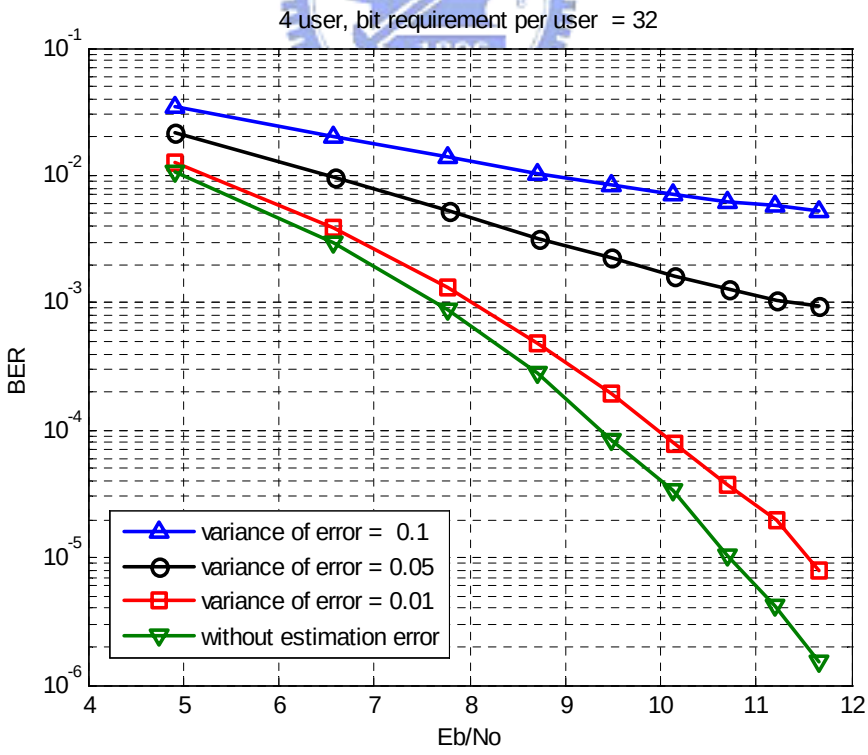

Figure 5.5: BER performances of beamforming aided multiuser resource allocation with channel estimation error

5.4 Summary

In this chapter we combine the two algorithms introduced in Chapter 3 and Chapter 4 in order to adaptively adjust our physical layer parameters including transmit and receive beamforming vectors, subcarriers, modulation orders and power. The algorithm is called beamforming aided multiuser adaptive radio resource management while frequency, time, space and multiuser diversities are used to enhance the overall system performance. The objective of the algorithm is to minimize the total transmit power while satisfying each users' QoS constraints. In multiuser adaptive MIMO-OFDM system, perfect CSI is essentially known in the transmitter. Therefore we introduce a signaling model for TDD based system in Section 5.2 and then BER performances with or without channel estimation error are shown in Section 5.3. It can be demonstrated that the results of beamforming aided multiuser radio resource management perform well in power efficiency.

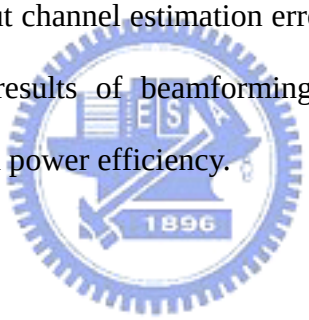

Chapter 6

Conclusion

In this thesis, the multiuser adaptive MIMO-OFDM system incorporating beamforming aided multiuser adaptive radio resource management algorithm is proposed. This algorithm can be divided into two parts. The first part is the beamforming aided subcarrier allocation algorithm which designs transmit and receive beamforming to let each subcarrier be occupied by more than one user without interference and solves the subcarrier assignment problem which chooses the users with better channel gain to transmit signal. The second part is a new bit and power allocation algorithm which obtains the optimum bit distribution with less computational complexity.

In Chapter 3, the ZF beamforming design algorithm is presented first. This algorithm uses the channel state information and SVD to jointly design transmit and receive beamformers. The transmit beamforming vector tries to match independent subchannels that are produced from the channel composed of allowed users' channel matrices. The function of the receive beamforming vector is to null interference from other users. Based on the beamforming design, we can calculate the output SNR of for each user. In order to maximize the total system performance, a beamforming aided subcarrier allocation algorithm is proposed. By some derivations, we find that the

throughput of the single carrier system is proportional to the product of the SNRs of all allowed users if each user's BER constraint is the same. Consequently, we choose the product of SNRs as the metric while selecting users to transmit data in one subcarrier. The group of users can utilize this subcarrier only if the product of SNRs for these users is the largest. As soon as which users can occupy each subcarrier is decided, which subcarriers can be used by one user also can be decided. Through judiciously assigning subcarriers to users, the overall transmission rate of the multiuser MIMO-OFDM system can be increased.

After the beamforming aided subcarrier allocation algorithm is introduced, the two-stage optimal bit and power loading algorithm is presented in Chapter 4. Under the QoS constraints including rate and BER requirements, this algorithm aims to minimize the total transmit power. For instance, the subcarriers with good channel qualities are more likely to employ a higher modulation order to reduce the overall transmit power of the system, while the subcarriers with poor channel qualities are more likely to employ a lower modulation order to maintain the target BER. The algorithm can find the optimal bit distribution with lower computational power compared with other algorithms. This algorithm is divided into two stages. The core idea of the first stage is to utilize the difference of CNRs between subcarriers to calculate an initial bit allocation. The result shows it has no more than a single bit difference per subcarrier compared with the optimal distribution. In the second stage, a bit-removal algorithm with fewer candidates is used to achieve the target rate bit distribution. It can be demonstrated that this algorithm works well in saving total transmit power with users' rate constraints satisfied. Finally, the complexity analysis shows that the proposed algorithm needs less computational operations compared with other conventional algorithms.

In Chapter 5, we combine the two algorithms introduced in Chapter 3 and Chapter

4 to adaptively adjust physical layer parameters including transmit and receive beamforming vectors, subcarriers, modulation orders and transmit power. The ultimate goal is to minimize the total transmit power in the system while satisfying each user's QoS. The algorithm is called beamforming aided multiuser adaptive radio resource management; it can fully use frequency, time, space and multiuser diversity to enhance the overall system performance. In multiuser adaptive MIMO-OFDM systems, perfect channel state information is essentially known in the transmitter. Therefore a signaling model for TDD based system is given. However, in practice it is impossible to obtain perfect CSI due to noisy channel estimation and unavoidable delay between performing channel estimation and using estimation result for actual transmission. Hence we show BER performances with channel estimation error and observe that the performance degradation is acceptable when the error variance is less than 0.01.

Furthermore, if we design the problem without perfect CSI but with partial state information, the results may be more suited for practical systems. In recent research, partial CSI issue has been considered important. Based on the partial CSI, the future work can be directed toward the re-design of beamforming aided subcarrier allocation and adaptive bit and power loading algorithms suited to multiuser MIMO-OFDM systems.

Bibliography

[1] V. Tarokh, H. Jafarkhani, and A. R. Calderbank, “Space-time codes for high data rate wireless communication: performance criterion and code construction,” *IEEE Trans. Inf. Theory*, vol. 44, no. 2, pp. 744–765, Mar. 1998.

[2] “Space-time block codes from orthogonal designs,” *IEEE Trans. Inf. Theory*, vol. 45, no. 5, pp. 1456–1467, Jul. 1999.

[3] S. M. Alamouti, “A simple transmit diversity technique for wireless communications,” *IEEE J. Sel. Areas Comm.*, vol. 16, no. 10, pp. 1451–1458, Oct. 1998.

[4] D.P. Palomar, J. M. cioffi and M. A. Lagunas, ‘Joint Tx-Rx beamforming design for multicarrier MIMO channels: a unified framework for convex optimization,” *IEEE Trans. Signal Processing*., vol. 51, pp. 2381-2401, no 9, Sept. 2003

[5] D.P. Palomar and M. A. Lagunas, “Joint transmit-receive space-time equalization in spatially correlated MIMO channels: a beamforming approach,” *IEEE J. Sel. Areas*., vol 21, pp 730-743, no 5, June 2003

[6] P. A. Dighe, R. K. Mallik, and S. S. Jamuar, “Analysis of transmit-receive diversity in Rayleigh fading,” *IEEE Trans. Comm.*, vol. 51, no. 4, pp. 694–703, Apr. 2003.

[7] S. Thoen, L. V. der Perre, B. Gyselinckx, and M. Engels, “Performance analysis of combined transmit-SC/receive-MRC,” *IEEE Trans. Comm.*, vol. 49, no. 1, pp. 5–8, Jan. 2001.

[8] C.-H. Tse, K.-W. Yip, and T.-S. Ng, “Performance tradeoffs between maximum ratio transmission and switched-transmit diversity,” in *Proc. IEEE PIMRC*, vol. 2, Sept. 2000, pp. 1485–1489.

[9] R. W. Heath Jr. and A. Paulraj, “A simple scheme for transmit diversity using partial channel feedback,” in *Proc. IEEE Asilomar Conf. Signals, Syst., Comput.*, vol. 2, Nov. 1998, pp. 1073–1078.

[10] M. Kang and M. S. Alouini, “Largest eigenvalue of complex wishart matrices and performance analysis of MIMO MRC systems,” *IEEE J Sel. Areas Comm.*, vol. 21, no. 4, pp. 418–426, Apr. 2003.

[11] H. Shi, M. Katayama, T. Yamazato, H. Okada, and A. Ogawa, “An adaptive antenna selection scheme for transmit diversity in OFDM systems,” in *Proc. IEEE Veh. Technol. Conf. Fall*, vol. 4, Oct. 2001, pp. 2168–2172.

[12] Xing Zhang; Wenbo Wang; Yuanan Liu; “Multiuser OFDM with adaptive frequency-time two-dimensional wireless resource allocation**”** *IEEE J Sel. Areas Comm.*, vol 2, Aug.-1 Sept. 2004 pp.824 - 828

[13] Zukang Shen; Andrews, J.G.; Evans, B.L., ”Adaptive resource allocation in multiuser OFDM systems with proportional rate constraints”, *IEEE Trans. Wireless Comm.*, vol. 4, issue 6, Nov. 2005 pp. 2726 – 2737

[14] Ying Jun Zhang; Letaief, K.B.;, “Multiuser adaptive subcarrier-and-bit allocation with adaptive cell selection for OFDM systems” *IEEE Trans. Wireless Comm,*. vol. 3, Issue 5, Sept. 2004 pp.1566 - 1575

[15] S. Catreux, D. Gesbert, V. Ercge and R. W. Heath JR, “Adaptive modulation and MIMO coding for broadband wireless data networks,” *IEEE Comm. Mag..*, Jun. 2002.

[16] G. G. Raleigh and J. M. Cioffi, “Spatio-temporal coding for wireless communication,” *IEEE Trans. Comm.*, vol. 46, pp. 357-366, Mar. 1998.

[17] H. Sampath, S. Talwar, J. Tellado, V. Erceg, and A. Paulraj, “A fourth-generation MIMO-OFDM broadband wireless system: design, performance, and field trial results,” *IEEE Comm. Mag.*, vol. 40, no. 9, pp. 143-149, Sep. 2002.

[18] T. S. Rappaport, A. Annamalai, R. M. Buehrer, and W. H. Tranter, “Wireless communications: past events and a future perspective,” *IEEE Comm. Mag.*, vol. 40, no. 5, pp. 5-14, May. 2002.

[19] R. Knopp and P. A. Humblet, “Information capacity and power control in single-cell multiuser communications,” *Proc. IEEE ICC’95*, pp. 331-335, Jun. 1995.

[20] C. Wong, R. Cheng, K. Letaief, and R. Murch, “Multiuser OFDM with adaptive subcarrier, bit, and power allocation,” *IEEE J. Select. Areas Commun.*, vol. 17, no. 10, pp. 1747-1758, Oct. 1999.

[21] D. Kivanc and H. Lui, “Subcarrier allocation and power control for OFDMA,” *Conf. on Signals, Systems, and Computers*, vol. 1, pp. 147–151, 2000.

[22] H. Sampath, S. Talwar, J. Tellado, V. Erceg, and A. Paulraj, “A fourth-generation MIMO-OFDM broadband wireless system: design, performance, and field trial results,” *IEEE Comm. Mag.*, vol. 40, no. 9, pp. 143-149, Sep. 2002.

[23] T. S. Rappaport, A. Annamalai, R. M. Buehrer, and W. H. Tranter, “Wireless communications: past events and a future perspective,” *IEEE Comm. Mag.*, vol. 40, no. 5, pp. 5-14, May. 2002.

[24] H. Yang, “A road to future broadband wireless access: MIMO-OFDM-based air interface,” *Bell Labs Syst. Tech. J.*, vol. 1, pp. 41-59, Autumn 1996.

[25] R. D. Murch and K. B. Letaief, “Antenna systems for broadband wireless access,” *IEEE Commun. Mag.*, vol. 40, pp. 76–83, Apr. 2002.

[26] G. G. Raleigh and J. M. Cioffi, “Spatio–temporal coding for wireless communications,” *IEEE Trans. Comm.*, vol. 46, pp. 357–366, Mar. 1998.

[27] P. Vandenameele, L. V. D. Perre, M. G. E. Engels, and H. J. D. Man, “A combined OFDM/SDMA approach,” *IEEE J. Sel. Areas Comm.*, vol. 18, pp. 2312–2321, Nov. 2000.

[28] J. Kim and J. Cioffi, “Spatial multiuser access with antenna diversity using singular value decomposition,” *in Proc. IEEE ICC*, vol. 3, 2000, pp. 1253–1257.

[29] P. J. Smith and M. Shafi, “On a Gaussian approximation to the capacity of wireless MIMO systems,” *Proc. IEEE ICC’02*, vol. 1, no. 28, pp. 406-410, May. 2002.

[30] G. J. Foschini, “Layered space-time architecture for wireless communication in a fading environment when using multiple antennas,” *Bell Labs Syst. Tech. J.*, vol. 1, pp. 41-59, Autumn 1996.

[31] G. J. Foschini and M. J. Gans, “On limits of wireless communications in a fading environment when using multiple antennas,” *Wireless Personal Comm.*, vol. 6, no. 3, pp. 311-335, 1998.

[32] P. W. Wolniansky, G. J. Foschini, G. D. Golden, and R. A. Valenzuela, “V-BLAST: an architecture for realizing very high data rates over the rich-scattering wireless channel,” *URSI International Symposium*, pp. 295-300, Oct. 1998.

[33] G. J. Foschini, G. D. Golden, R. A. Valenzuela, and P. W. Wolniansky, “Simplified processing for high spectral efficiency wireless communication employing multi-element arrays,” *IEEE J. Select. Areas Comm.*, vol. 17, no. 11, pp. 1841-1852, Nov. 1999.

[33] V. Tarokh, N. Seshadri, and A. R. Calderbank, “Space-time codes for high data rate wireless communication: performance analysis and code construction,” *IEEE Trans. Inform. Theory*, vol. 44, no. 2, pp. 744-765, Mar. 1998.

[34] V. Tarokh, H. Jafarkhani, and A. R. Calderbank, “Space-time block codes from orthogonal designs,” *IEEE Trans. Inform. Theory*, vol. 45, no. 5, pp. 1456-1467, July 1999.

[35] V. Tarokh, H. Jafarkhani, and A. R. Calderbank, “Space-time block coding for wireless communications: performance results,” *IEEE J. Select. Areas Comm.*, vol. 17, no. 3, pp. 451-460, Mar. 1999.

[36] P. Vandenaeele, L. V. D. Perre, M. G. E. Engels, and H. J. D. Man, “A combined OFDM/SDMA approach,” *IEEE J. Sel. Areas Comm.*, vol. 18 pp. 2312-2321, Nov. 2000

[37] J. Kim and J. Cioffi, “Spatial multiuser access with antenna diversity using singular value decomposition,” *in Proc. IEEE ICC*, vol. 3, 2000, pp. 1253-1257

[38] W. Yu, W. Rhee, and J. M. Cioffi, “Optimal power control in multiple-access fading channels with multiple antennas,” *in Proc. IEEE ICC*, vol.2, 2001, pp. 575-579

[39] G. V. Klimovitch, ‘Maximizing data rate-sum over vector multiple access channel,” *in Proc. IEEE WCNC*, vol. 1, 2000, pp. 287-292

[40] S. T. Chung, and A. J. Goldsmith, “Degrees of freedom in adaptive modulation: a unified view,” *IEEE Trans. Comm*. vol.49, no. 9, Sept 2001, pp.1561-1571

[41] P. S. Chow, J. M. cioffi, and J. A. C. Bingha m, “A practical discrete multitone transceiver loading algorithm for data transmission over spectrally shaped channels,” *IEEE Trans. Comm.*, vol. 32, no. 2-4, pp. 773-775, Feb./Mar./Apr. 1995

[42] A. Leke and J. M. Cioffi, ”A maximum rate loading algorithm for discrete multitone modulation systems,” in *Proc. IEEE Globelcom*, vol. 3, Nov. 1997, pp. 1514-1518

[43] E. baccarelli, A. Fasano, and M. Biagi, “Novel efficient bit-loading algorithms for peak-energy-limited ADSL multicarrier systems,” *IEEE Trans. Signal Process*., vol. 50, no. 5, pp. 1237-1247, May 2002.

[44] J. Campello, “Practical bit loading for DMT,” *in Proc. IEEE IEE*, vol. 2, Jun. 1999, pp. 801-805

[45] R. V. Sonalkar and R. R. Shively, “An efficient bit-loading algorithm for DMT applications,” *IEEE Trans. Comm. Lett.*, vol. 4, no. 3, pp. 80-82 , Mar. 2000.

[46] T. Keller and L. Hanzo, “Adaptive modulation techniques for duplex OFDM transmission,” *IEEE Trans. Veh. Technol.*, vol 49, pp. 1893-1906, Sep. 2000.

[47] Y. J. Zhang and K. B. Letaief, “Adaptive resource allocation for multiaccess MIMO/OFDM systems with matched filtering,” *IEEE Trans. Comm*. vol 53, no.11, pp.1810-1816, Nov. 2005

[48] N. Papandreou and T Antonakopoulos, “A new computationally efficient discrete bit-loading algorithm for DMT applications,” *IEEE Trans. Comm.*, vol.53, no.5, pp.785-789, May. 2005

[49] W. Rhee, W. Yu and J. M. Cioffi, “The optimality of beamforming in uplink multiuser wireless systems,” *IEEE Trans. Wireless Comm*., vol 3, no.1, pp.86-96, Jan. 2004

[50] A. Fasano, “On the optimal discrete bit loading for multicarrier systems with constraints,” *in Proc. IEEE VTC*, pp. 915-919. April 2003

[51] A. G. Armada, “SNR gap approximation for M-PSK based bit loading,” *IEEE Trans. on Wireless Comm*, vol.5, no. 1, Jan. 2006

[52] Y. Yingwei, G. B. Giannakis, “Rate-maximizing power allocation in OFDM based on partial channel knowledge,” *IEEE Trans. wireless commun.*, vol. 4, no. 3, pp. 1073-1083, May 2005.

[53] A. Fasano, G. Di Blasio, E. Baccarelli, and M. Biagi, “Optimal discrete bit loading for DMT based constrained multicarrier systems,” *in Proc. IEEE ISIT*, Jul. 2002, p. 243.

[54] E. Baccarelli and M. Biagi, “Optimal integer bit-loading for multicarrier ADSL systems subject to spectral-compatibility limits,” *Signal Process*.; vol. 84, pp. 729-741, Apr. 2004